Endostructural morphology in hominoid mandibular third premolars: Discrete traits at the enamel-dentine junction

Thomas W. Davies[a,b,*], Lucas K. Delezene[c], Philipp Gunz[b], Jean-Jacques Hublin[b], Matthew M. Skinner[a,b]

[a] *School of Anthropology and Conservation, University of Kent, Canterbury, CT2 7NZ, UK*

[b] *Department of Human Evolution, Max Planck Institute for Evolutionary Anthropology, Deutscher Platz 6, 04103 Leipzig, Germany*

[c] *Department of Anthropology, University of Arkansas, Fayetteville, Arkansas, 72701 USA*

*Corresponding author.

E-mail address: thomas_davies@eva.mpg.de (T.W. Davies)

Keywords: Premolars; Enamel-dentine junction; Discrete traits; Dental development; Taxonomy; Dental morphology

Acknowledgements

For access to specimens, we would like to thank Bernhard Zipfel, Lee Berger, Sifelani Jira (Evolutionary Studies Intitute, University of the Witwatersrand), Miriam Tawane (Ditsong Museum), Job Kibii (National Museums of Kenya), Metasebia Endalemaw, Yared Assefa (Ethiopian Authority for Research and Conservation of Cultural heritage), Yoel Rak, Alon Barash, Israel Hershkovitz (Sackler School of Medicine), Michel Toussaint (ASBL Archéologie Andennaise, Jean-Jacques Cleyet-Merle (Musée National de Préhistoire des Eyzies-de-Tayac), Ullrich Glasmacher (Institut für Geowissenschaften, Universität Heidelberg), Robert Asher, Hendrik Turni, Irene Mann (Museum für Naturkunde, Berlin), Jakov Radovčić (Croatian Natural History Museum), Christophe Boesch and Uta Schwarz (Max Planck Institute for Evolutionary Anthropology) and the Leipzig University Anatomical Collection (ULAC). For project support we thank Zeresenay Alemseged and Bill Kimbel. We would also like to thank the reviewers, the associate editor and the editor for their helpful comments and guidance, as well as Ottmar Kullmer for comments on an earlier version of this manuscript. This work was funded by the Max Planck Society, and financial support for L.K.D. was provided by a Connor Family Faculty Fellowship and the Office of Research and Development at the University of Arkansas.

Endostructural morphology in hominoid mandibular third premolars: Discrete traits at the enamel-dentine junction

Abstract

The mandibular third premolar (P_3) exhibits substantial differences in size and shape among hominoid taxa, and displays a number of discrete traits that have proven to be useful in studies of hominin taxonomy and phylogeny. Discrete traits at the enamel-dentine junction (EDJ) can be accurately assessed on moderately worn specimens, and often appear sharper than at the outer-enamel surface (OES). Here we use microtomography to image the P_3 EDJ of a broad sample of extant apes, extinct hominins and modern humans (n = 100). We present typologies for three important premolar discrete traits at the EDJ (transverse crest, marginal ridge and buccal grooves), and score trait frequencies within our sample. We find that the transverse crest is variable in extant apes, while the majority of hominins display a transverse crest which runs directly between the two major premolar cusps. Some Neanderthals display a unique form in which the transverse crest fails to reach the protoconid. We find that mesial marginal ridge discontinuity is common in *Australopithecus anamensis* and *Australopithecus afarensis* while continuous marginal ridges largely characterize *Australopithecus africanus* and *Paranthropus*. Interrupted mesial and distal marginal ridges are again seen in *Homo sapiens* and Neanderthals. Premolar buccal grooves, previously identified at the OES as important for hominin systematics, are again found to show a number of taxon-specific patterns at the EDJ, including a clear difference between *Australopithecus* and *Paranthropus* specimens. However, their appearance may be dependent on the morphology of other parts of the crown such as the protoconid crest, and the presence of accessory dentine horns. Finally, we discuss rare variations in the form of dentine horns that underlie premolar cusps, and their potential homology to similar morphologies in other tooth positions.

1. Introduction

Teeth are an important component of the fossil record; as highly mineralized and compact tissues, they are well preserved and, therefore, common in fossil deposits. They are also a rich source of information regarding taxonomy, diet, and environment, among other factors (Walker et al., 1978; Sponheimer and Lee-Thorp, 1999; Richards et al., 2001; Lee-Thorp et al., 2003; Grine et al., 2012). Unlike bones, the external morphology of the tooth crown is not remodeled throughout life; once fully developed, it is only modified by external factors such as breakage or wear. Further, aspects of tooth morphology show high levels of heritability (Townsend and Martin, 1992; Dempsey and Townsend, 2001; Hlusko and Mahaney, 2003) and dental traits are considered particularly useful in studies of taxonomy and phylogeny (Wood and Abbott, 1983, Wood et al., 1983; Suwa et al., 1996; Irish and Guatelli-Steinberg, 2003).

Many previous studies of the hominin dentition have focussed on molars, since they are the most morphologically complex teeth, while premolars are considered transitional teeth between the simple, single-cusped canines and the more complex, multi-cusped molars. Premolars are extremely variable, however, and can show a variety of morphologies even among hominoids (e.g., Davies et al., 2019). This is especially true of the mandibular third premolar (P_3), which forms part of the catarrhine canine honing complex (e.g., Walker, 1984; Greenfield and Washburn, 1992; Delezene, 2015). As a result of substantial reduction in maxillary canine height, hominins are the only catarrhine clade in which the function of canine honing has been lost (e.g., Greenfield, 1990; Brunet et al., 2002; Haile-Selassie et al., 2004; Suwa et al., 2009). The loss of canine honing may have removed a functional constraint on P_3 morphology that permitted the evolution of novel P_3 forms among hominins.

Intraspecific P_3 variability was noted by Kraus and Furr (1953), who outlined 17 traits in modern humans that relate to the development and position of the major cusps, the form of major occlusal ridges, and the presence of features such as buccal grooves. Wood and Uytterschaut (1987) built upon these definitions to study mandibular premolar variation among Plio-Pleistocene hominins, noting for example that cusp number is effective in distinguishing between *Paranthropus* and other hominins, while the position of the lingual cusp can be used to distinguish eastern African *Homo*. Further, Suwa (1988) identified a number of P_3 features that distinguish *Paranthropus* from other hominins and Suwa et al. (1996) outlined derived P_3 features of early *Homo* and *Australopithecus africanus*, relative to *Australopithecus afarensis*, as well as those unique to early *Homo*. P_3 traits have also been utilized in studies of *Ardipithecus* (Haile-Selassie et al., 2004; Suwa et al., 2009), *Australopithecus anamensis, A. afarensis* (Leonard and Hegmon, 1987; Ward et al., 2001; Kimbel et al., 2006; Delezene and Kimbel, 2011) and *Homo naledi* (Irish et al., 2018).

Nonmetric features are typically assessed at the outer-enamel surface (OES); however, advances in microtomography allow the assessment of internal tooth structures. Of particular interest in studying discrete dental traits is the enamel-dentine junction (EDJ). The EDJ preserves the form of the basement layer of the inner-enamel epithelium, the morphology of which is determined during odontogenesis. Subsequently, enamel and dentine are deposited on either side of this epithelial layer, meaning that important OES dental features such as cusps and crests typically originate at the EDJ (Skinner et al., 2008 and references therein). The advantages of studying the morphology of the EDJ are twofold. Firstly, tooth wear can prevent assessment of discrete dental traits (Burnett et al., 2013); however, the EDJ is preserved in specimens with moderate wear, allowing assessment of specimens that would otherwise be excluded from analyses. Secondly, hominin teeth often have thick enamel (Beynon and Wood, 1986; Macho and Thackeray, 1992; Smith et al., 2012; Skinner et al.,

2015), which may make the exact form and layout of crown features difficult to assess. In contrast, features at the EDJ appear much sharper, allowing for more accurate and precise trait assessment. As a result, although the OES and EDJ have a high level of correspondence (Nager, 1960; Skinner et al., 2010; Ortiz et al., 2012; Morita et al., 2014; Guy et al., 2015), trait-scoring systems developed for the OES may not always be applicable when studying the EDJ.

Various studies have investigated the expression of discrete molar traits at the EDJ (e.g., Korenhof, 1960; Corruccini, 1987; Skinner et al., 2008; Anemone et al., 2012; Zanolli and Mazurier, 2013; Martinón-Torres et al., 2014; Martínez de Pinillos et al., 2014; Zanolli, 2015; Martin et al., 2017; Liao et al., 2019), which help to understand the range of variation in the form of these traits. Studying the EDJ also allows us to better understand the development of dental traits so that we can accurately identify traits and their covariation with one another, or with other aspects of crown morphology, both of which can be important when using traits to make taxonomic arguments. Fewer studies have explored discrete premolar traits at the EDJ, although a number of studies have done so alongside molars (e.g., Braga et al., 2010; Liu et al., 2013; Zanolli et al., 2018). Sakai (1967) studied the modern human P_3 using destructive techniques to view the EDJ and explore the expression of discrete traits such as buccal grooves and an indentation on the mesial marginal ridge termed a 'trigonid notch'. The form of these traits was compared to the morphology of the OES, and discussed with reference to what was known about the expression of these traits at the OES of fossil hominins. Further, Krenn et al. (2019) studied modern human mandibular premolars at the EDJ and OES, scoring the variation in seven different qualitative traits including the form of the marginal ridges, the extension of the transverse crest, and the number of accessory crests present on the crown, finding inter-population differences in a number of traits. Despite advances in microtomography allowing the non-destructive imaging of internal tooth structures in fossils,

100 no study has yet explored the EDJ expression of P_3 discrete traits across the hominin clade.
101 Here we examine the P_3 EDJ of a broad sample of extant apes, modern humans and extinct
102 hominins, focussing on three important discrete traits that are variable within this sample. We
103 present scoring systems for these traits, and discuss the concordance (or lack thereof) with
104 traits previously scored at the OES. We score trait frequencies within our sample to identify
105 features that may have taxonomic significance, and discuss the developmental basis of a
106 number of these traits.

107 A second companion paper will use geometric morphometrics to quantitatively analyze
108 hominoid P_3 EDJ morphology (Davies et al. 2019).

109

110 **2. Methods**

111 *2.1 Study sample*

112 The sample is summarized in Table 1 (a full list of specimens can be found in
113 Supplementary Online Material [SOM] Table S1) and consists of 100 specimens, of which 93
114 are assigned to species rank. Two specimens are assigned to *Homo* sp., and five are
115 considered indeterminate. The recent *H. sapiens* sample is curated at the University of Leipzig
116 Anatomical Collection (ULAC). Relatively little information is available on the provenance
117 of this sample, but the available information is presented in SOM Table S2. The study sample
118 is limited by the availability of microtomographic scans and the ability to extract the EDJ
119 surface from those scans. The EDJ surface is more difficult to extract in some cases due to a
120 lack of radiographic tissue contrast between enamel and dentine; this problem is more
121 prevalent at eastern African sites (although the taphonomic processes that are likely causing
122 this are not clear), and the sample sizes for taxa known mostly from these sites (e.g.,
123 *Paranthropus boisei*, *A. anamensis*, *A. afarensis*, and early *Homo*) are more limited. Further,
124 the physical preservation of the fossils is important, and specimens that are heavily cracked,

125 eroded or otherwise broken often have to be excluded from analyses when digital
126 reconstruction is not possible. Scan resolution is also important to consider: larger traits such
127 as main cusps and crests remain visible at the entire range of scan resolutions used; however,
128 smaller features such as accessory cusps can be difficult to identify at lower resolutions,
129 particularly in poorer quality scans. Scan resolution is limited by a number of factors
130 including the shape and size of the specimen, as this limits how closely the specimen can be
131 placed to the X-ray source, as well as the time available for scanning. Nonetheless, the sample
132 does capture a broad swath of the hominin clade, including modern humans, and includes
133 representatives of all extant apes as comparative outgroups. Given sample size constraints, it
134 is very likely that this study does not capture the full extent of P_3 variation in each taxon;
135 however, the trait scoring systems outlined can be expanded as necessary.

136

137 *2.2 Microtomography and segmentation*

138 Microtomographic scans of P_3 sample were obtained using either a SkyScan 1173 at 100–
139 130 kV and 90–130 μA, a BIR ACTIS 225/300 scanner at 130 kV and 100–120 μA, or a
140 Diondo d3 at 100–140kV and 100–140 μA, and reconstructed as 8-bit TIFF stacks (isometric
141 voxel resolutions ranging from 13–45 μm). TIFF stacks were filtered using 3D median filter,
142 followed by a mean of least variance filter (each with a kernel size of either one or three),
143 implemented using MIA open source software (Wollny et al., 2013). Filtered image stacks
144 were segmented using Avizo 6.3 (Visualization Sciences Group, 2010) to produce PLY
145 format surface models of the EDJ. The EDJ of specimens with substantial cracks were
146 realigned using Geomagic Studio 2014 (3D systems, Rock Hill) when possible.

147

148 *2.3 Scoring procedures*

149 The presence and form of four EDJ discrete traits were scored; the transverse crest,
150 marginal ridge continuity, mesial buccal groove and distal buccal groove. While each of these
151 traits has been previously described at the OES for hominoids, the extent of variation in these
152 traits at the EDJ has not been previously described. These traits were chosen because initial
153 investigations showed that they are variable within our sample, and are able to be scored in a
154 way that is both precise and reproducible. Since traits were only scored at the EDJ, and not at
155 the OES, discussion of the form of these traits refers to the EDJ, unless otherwise specified.

156 In addition to these four traits, unusual dentine horn morphologies were recorded when
157 present and, although not formally scored, the presence of accessory cusps is noted.
158 Intraobserver error was assessed through the rescoring of the entire sample by the primary
159 observer (T.W.D.) more than one month after the initial scoring. Interobserver error was
160 assessed through a second observer (M.M.S.) scoring a subset of 25 specimens for each trait.
161 Inter- and intraobserver agreement was high, and errors appear to be random as they are not
162 limited to specific taxa or trait types; results of the observer error tests can be found in SOM
163 Table S3.

164 Transverse crest A number of authors have considered aspects of premolar transverse crest
165 form at the OES (Suwa, 1990; Leonard and Hegmon, 1987; Bailey, 2002; Delezene and
166 Kimbel, 2011, Irish et al., 2018). Some focussed on the prominence of the transverse crest
167 (Suwa, 1990; Bailey, 2002; Irish et al., 2018), while others preferred to score the orientation
168 of the transverse crest (Delezene and Kimbel, 2011). Leonard and Hegmon (1987) previously
169 scored a number of *A. afarensis* P_3 specimens for 'transverse ridge development', using a
170 five-point typology, which attempted to score both the form and prominence of the P_3
171 transverse crest. In a modern humans, Krenn et al. (2019) scored whether or not the transverse

crest is bifurcated, as well as whether it runs continuously between the two cusps or is interrupted.

When studying the hominoid transverse crest at the EDJ, it is apparent that the relationship between this crest and other crown structures, particularly the main premolar cusps, is highly variable. Therefore the typology used here focuses on the position of the transverse crest relative to other crown structures, and is based on the range of variation observed within the present sample. Unlike previous studies, the scoring system does not aim to characterize how strongly developed the transverse crest is (beyond presence/absence) because this is difficult to score objectively.

The scoring procedure consists of five discrete categories (although Types 1 and 1a are related) as follows (Fig. 1): Type 0 = transverse crest is absent, or only small incipient crests are present; Type 1 = transverse crest is present, and connects the protoconid to the metaconid (or equivalent point on the marginal ridge, when a clear metaconid is not present); Type 1a = transverse crest connects to the lingual margin of the tooth, but flattens to the level of the surrounding occlusal basin before connecting to the protoconid; Type 2 = transverse crest connects to the protoconid, but is either deflected distally or flattens to the level of the occlusal basin before connecting to the marginal ridge on the lingual side of the tooth; Type 3 = transverse crest connects to the protoconid crest distal to the dentine horn tip and, as in Type 2, is either deflected distally or flattens to the level of the surrounding occlusal basin before connecting to the marginal ridge on the lingual side of the tooth.

In some specimens, particularly those with tall well-developed dentine horns, the transverse crest may appear not to reach the dentine horn tip or adjacent crest, being flattened to the level of the surrounding dentine such that the ridge is no longer visible. Here, the transverse crest was considered associated to the dentine horn provided that the crest is visible for at least two-thirds of the dentine horn height. Therefore, Type 1a is reserved for specimens

in which the transverse crest is flattened for more than one-third the height of the protoconid, as measured from the tip of the protoconid to the bottom of the occlusal basin. This distinction is illustrated in Figure 1 when comparing Neanderthal specimens KRP 51 (Type 1) with KRP D33 and KRP D114 (Type 1a). The distinction between Types 2 and 3, in the case of a partly flattened transverse crest, was made by judging whether the remaining portion of the crest is angled such that, were it to be present for the full length of the crown, it would make contact with the tip of the protoconid or with the adjacent crests. Specimens that have been digitally reconstructed due to tooth wear have been included in this analysis provided we could be confident of the form of the transverse crest, and provided the reconstructed portion makes up no more than 1/3 of the height of the dentine horn. The expression of any additional crests present in the occlusal basin of the tooth will also be discussed. It should be noted that although Type 1a is classed as a subtype of Type 1 (an explanation for this can be found in the discussion), we refer to these types separately, unless otherwise stated.

Marginal ridge continuity One difference between the P_3 of hominins and apes is that hominins typically have more strongly developed distal and mesial marginal ridges (Suwa, 1990). However, even among hominins the prominence and form of the marginal ridge varies; this variation has been considered by a number of authors (Suwa, 1990; Ward et al., 2001). In particular, it has been noted that the mesial marginal ridge is often poorly developed in early hominins; such specimens are described as having an 'open mesial fovea' (Kimbel et al., 2006; Delezene and Kimbel, 2011).

Further, Sakai (1967) noted the presence of a 'trigonid notch' in the P_3 EDJ of modern humans, defined as a clear indentation in the mesial marginal ridge, and Krenn et al. (2019) scored modern human premolars for missing or reduced marginal ridges at the EDJ and OES. In our sample, specimens may exhibit a morphology resembling the trigonid notch described by Sakai (1967), or they may show poorly developed, or absent, marginal ridges on the mesial

222 or distal side of the crown. Since the difference between a 'notched' marginal ridge and one
223 that is poorly developed may be very slight, the grading system used here instead scores
224 marginal ridge continuity (or discontinuity), where a discontinuous marginal ridge is one
225 which is flattened to the level of the occlusal basin for some portion of its length. This system
226 therefore does not distinguish between absent, poorly developed and notched marginal ridges.
227 Marginal ridge continuity was scored on the mesial and distal marginal ridges, according to
228 the following system (Fig. 2): C = continuous marginal ridges; the distal marginal ridge runs
229 from the distal protoconid crest to the metaconid (or equivalent point on the crown), and the
230 mesial marginal ridge runs from this point, to the mesial protoconid crest; M = the mesial
231 marginal ridge is discontinuous; D = the distal marginal ridge is discontinuous; MD = the
232 mesial and distal marginal ridges are both discontinuous.

233 Marginal ridges may appear to flatten to the level of the occlusal basin at the base of the
234 metaconid dentine horn, but this was only counted as discontinuous if the flattened section
235 clearly extended further into the mesial or distal fovea than the base of the metaconid. This
236 analysis was only completed on hominin specimens, excluding the extant apes, since the
237 mesial and distal marginal ridges are generally poorly developed in extant apes.

238 Buccal grooves Kraus and Furr (1953:562), in their description of the morphology of the
239 modern human P_3, described the occasional presence of "a ridge and accompanying shallow
240 vertical groove" on both the mesial and distal margins of the buccal face, but specified that
241 these features are more often absent than present. Typically termed 'buccal grooves', this
242 feature is argued to be particularly common in *A. africanus* (Robinson, 1956; Wood and
243 Uytterschaut, 1987; Suwa, 1990). Suwa (1990) scored the degree of expression of buccal
244 grooves in the modern human P_3 at the OES; distal buccal grooves were scored as 'strong',
245 'moderate' or 'trace/lacking', while a fourth category of 'ill-defined but with a significant
246 triangular depression' was included for mesial buccal grooves. Similarly, Sakai (1967) scored

247 the presence of ‘buccal ridges’ at the EDJ in a sample of modern human P_3 using three
248 categories: ‘pronounced’, ‘weak’ or ‘no ridge’. Here specimens were scored using a similar
249 system to these two studies, although the fourth category used by Suwa (1990) for mesial
250 buccal grooves was not included such that specimens were scored using the same procedure
251 for both mesial and distal EDJ buccal grooves (Fig. 3): 0 = absent; the EDJ buccal face shows
252 no distinct grooves; there may be a slight vertical ridge on the mesial or distal margin of the
253 buccal face, but it is not associated with a clear concavity; 1 = minor; a vertical ridge is
254 present on the EDJ surface, and is associated with a small but distinct concavity; 2 = marked;
255 the EDJ buccal surface shows a clear extended vertical ridge associated with a marked
256 concavity.

257 It should be noted that buccal grooves are usually directly associated with either the
258 protoconid crest or marginal ridges (often the intersection between the two); although, in
259 some cases they are located closer to the cervix and may show little or no development higher
260 up on the crown. We made no distinction between these types, and instead scored only how
261 strongly developed the grooves are.

262 Cusp form and frequency The protoconid is universally present in the hominoid P_3 and, in the
263 majority of cases, consists of a single raised, conic dentine horn. However, there are a limited
264 number of cases in which the protoconid departs from this form, and these examples will be
265 discussed. The presence of accessory cusps will be discussed briefly; however, premolar
266 accessory cusps can often be very small at the EDJ, and for some specimens with a lower scan
267 resolution and/or poor contrast between tissue types in the scan, the presence of accessory
268 cusps at the EDJ is not always clear. The frequency of these cusps will therefore not be
269 formally scored.

270

3. Results

3.1 Transverse crest

The form of the transverse crest was assessed for 71 specimens using the typology outlined in Figure 2; the results are shown in Table 2 (full results can be found in SOM Table S1). The majority of these display a Type 1 transverse crest (65%; 46/71), however this type is rare among extant apes, where it is only seen in *Pongo*. *Hylobates* specimens uniformly have deflected transverse crests, with some connecting to the protoconid (Type 2) and others connecting to the distal protoconid crest (Type 3). The *Gorilla* P_3 also shows a deflected transverse crest, but connects to the protoconid (Type 2). All five *Pan* specimens display a deflected transverse crest (or one which otherwise fails to reach the lingual margin of the tooth); 4/5 of these are not angled towards the tip of the protoconid (Type 3). Type 3 is only present among the extant apes, and only one hominin specimen displays a Type 2 transverse crest. 78% (40/51) of hominin specimens display a transverse crest that runs from the protoconid to the metaconid (or the equivalent point on the marginal ridge; Type 1), and all hominin species represented here show a Type 1 transverse crest in at least one specimen. Type 1a, in which the transverse crest connects to the marginal ridge but does not reach the protoconid, is seen exclusively in Neanderthal specimens; 4/9 specimens display this type, while the remainder are Type 1.

A special case is the modern human specimen ULAC 790. This individual has poorly developed mesial and distal marginal ridges and no metaconid, making attribution to our typology difficult. In this specimen, the transverse crest extends lingually from the protoconid to meet a small ridge, which may or may not be a section of distal marginal ridge, but is very poorly developed (the main portion of the distal marginal ridge is situated on the distal edge of the crown, and does not connect to the transverse crest at any point).

295 A number of specimens display crests in addition to the main transverse crest (Fig. 4). For
296 example, *A. africanus* and *P. robustus* frequently display small crests running distolingually
297 towards the center of the distal fovea. These crests typically meet the transverse crest at the
298 protoconid apex, although they may meet partway across the transverse crest and lingual to
299 the protoconid (e.g., SK 100). Accessory crests are sometimes present on the lingual side of
300 the tooth as well. For example, for DNH 46 a crest originates at the metaconid and runs
301 towards the center of the distal fovea, while SK 62 displays a similar crest on the lingual side
302 of the tooth that appears to originate at the distal marginal ridge. Moreover, Neanderthal
303 specimens frequently display accessory crests, either mesial or distal to the main transverse
304 crest, on the face of the tall protoconid crest (Fig. 4). These are variable in number, size and
305 position, and are also seen, albeit less frequently, in modern humans.

306

307 *3.2 Marginal ridge continuity*

308 There were 69 hominin specimens for which the continuity of the marginal ridge was
309 scored (Table 3; see full results in SOM Table S1). Of these, 70% (48/69) displayed a
310 continuous marginal ridge (Fig. 2). With one exception, *A. anamensis*, all hominin species
311 represented by three or more individuals have at least one specimen displaying a continuous
312 marginal ridge. *Australopithecus anamensis* is unique among the hominin sample; all three
313 specimens display a poorly developed mesial marginal ridge, scored as mesially
314 discontinuous. Three *A. afarensis* specimens were scored, of which two (A.L. 266-1 and A.L.
315 333w-1c) displayed a discontinuous mesial marginal ridge, and one (A.L. 333-10) displayed
316 an entirely continuous marginal ridge. KNM-WT 8556 and W8-978 also display continuous
317 marginal ridges.

318 *Australopithecus africanus* displays a range of marginal ridge forms, although the majority
319 are continuous (nine continuous, two mesially discontinuous and one distally discontinuous).

STW 401 is the only example of an *Australopithecus* P_3 within this sample of a discontinuous distal marginal ridge. This specimen is also noteworthy because the form of this trait differs from that seen in later hominin specimens, and is different from that often seen on the mesial marginal ridge in *Australopithecus*. In the majority of cases discontinuities in the marginal ridge appear on either side of the metaconid; the marginal ridge lowers and flattens before reaching the dentine horn. In this case, however, there are two portions of the distal marginal ridge present that overlap one another, but do not meet. Continuous mesial and distal marginal ridges are seen in all specimens of *Paranthropus*, *H. naledi*, as well as the probable early *Homo* specimen SKX 21204 and are the most common form in *A. africanus*. In contrast, for *H. sapiens* (fossil and recent), half of the specimens in the sample display a discontinuous mesial and/or distal marginal ridge. None of the Neanderthal specimens in our sample show distal marginal ridge discontinuity, but 31% (4/13) show discontinuity in the mesial marginal ridge. The P_3 of the Mauer mandible also shows both mesial and distal discontinuity, while the Cave of Hearths P_3 shows mesial marginal ridge discontinuity. In some cases (e.g., ULAC 171; Fig. 1b), the marginal ridge is mostly absent, with only small lingual deflections from the mesial and distal protoconid crests. Finally, this trait is not always consistent between antimeres—ULAC 58 displays a discontinuous mesial marginal ridge on the left P_3, but not the right.

3.3 Buccal grooves

Buccal grooves were scored for 95 specimens (Table 4; see full results in SOM Table S1). Of these, 66% (63/95) show some level of buccal groove expression (mesial and/or distal). Buccal grooves are less common in the extant apes. In our sample, no extant ape specimen showed marked buccal grooves, mesial or distal; although all *Gorilla* and *Pan* specimens show minor distal buccal grooves (minor mesial buccal grooves are also present in half of

these specimens). Conversely, all 19 scorable *Australopithecus* specimens, as well as KNM-WT 8556 and W8-978, showed either minor or marked buccal grooves on both the distal and mesial sides. Further, in all *Australopithecus* specimens in which the mesial and distal buccal grooves are unequal, it is always the mesial buccal groove which is more strongly expressed. The opposite pattern is evident in *Paranthropus*, where the distal buccal grooves are generally better developed, and, in fact, mesial buccal grooves are absent in 86% (12/14) of *Paranthropus* specimens. In this respect, Omo specimen L427-7 is unusual for *Paranthropus*, as previously noted by Suwa (1990), as the P_3 displays marked mesial and distal buccal grooves. SXK 21204, a specimen attributed to early *Homo* (Grine, 1989), shows marked mesial and minor distal buccal grooves. *Homo naledi* specimens show minor or absent buccal grooves on both mesial and distal sides. Among modern humans and Neanderthals, buccal grooves are less common; no specimen showed marked mesial or distal buccal grooves. Neither the Mauer P_3 nor the Cave of Hearths P_3 show any buccal grooves, while 43% (6/14) Neanderthal and 86% (12/14) *H. sapiens* specimens exhibit no buccal grooves at all. Neanderthal specimens more often show minor buccal grooves on the mesial side (57%; 8/14) than on the distal side (21%; 3/14).

3.4 Protoconid form

The variation observed in the form of the protoconid is shown in Figure 5. The majority of specimens display a single, conic protoconid dentine horn tip, and as such, only the exceptions will be listed here (Fig. 5A). In Neanderthals and modern humans, the protoconid dentine horn tip may be less pronounced due to the presence of tall mesial and distal protoconid crests, and in one specimen, ULAC 790, there is no clearly differentiated protoconid tip, only a well-developed ridge (Fig. 5B). A small number of specimens display a protoconid with a longitudinally expanded tip (Fig. 5C). This feature is seen in two *H. naledi*

specimens, UW 101-144 and UW 101-889, and their probable antimeres (UW 101-506 and UW 101-377, respectively), as well as one *Pan* specimen, MPITC 11800. In some cases, such as UW 101-377, it is clear that the expanded dentine horn actually consists of two semidistinct tips. In other cases, the tip simply appears as a flattened ridge; however, since this structure is very small, it is possible that the resolution of the scans may be insufficient to discern two individual peaks. In one modern human, ULAC 58, the tip of the protoconid is transversely expanded (Fig. 5D). The protoconid crest meets the protoconid on the buccal side of the tip, while the transverse crest meets it on the lingual side of the tip, but these two points are not coincident, and are connected by a short ridge. This feature is present in both antimeres, but is not present in any other P_3 within our sample.

3.5 Accessory cusps

Poor tissue contrast in a number of specimens inhibits proper characterization of the frequency and detailed morphology of small accessory cusps. However, a number of general observations can be made. Many hominin specimens display small accessory cusps at multiple locations along the distal and mesial marginal ridges. There is commonly a small dentine horn at the distobuccal corner of the tooth, at the intersection between the distal marginal ridge and the distal protoconid crest. This cuspulid can be seen in most hominin species, although it appears to be less common in modern humans and Neanderthals (issues of scan tissue contrast are less problematic in these specimens). It may be related to the presence of distal buccal grooves since the tip of the dentine horn is often contiguous with a raised ridge of dentine on the buccal face, while the concavity seen on the buccal face, immediately mesial to this ridge, is somewhat contiguous with the base of the dentine horn on the protoconid crest. A particularly pronounced example of this can be seen in STW 213 (Fig. 3). Accessory cusps are also found along the distal and mesial marginal ridges, and in some

cases, they can be nearly as large as the metaconid, as seen in L427-7. Other specimens, such as STW 151, display multiple accessory cusps, in this case along the distal marginal ridge.

4. Discussion

4.1 Transverse crest form

In the majority of hominins (78%; 40/51), the P_3 transverse crest extends lingually from the protoconid to meet the metaconid or equivalent point on the marginal ridge (Type 1; Fig. 1). This is rare in extant apes. In *Hylobates* and *Gorilla*, the transverse crest does not typically reach the weakly developed marginal ridge, either ending mesial to the ridge, or deflecting distally. All *Pan* specimens studied here fit within Type 2 or 3, although the form of the transverse crest is quite variable in shape; some specimens have small associated accessory crests, while others are raised high above the crown basin or may have raised sections. Given the level of variability in even our small sample, further investigation is required. Such studies should also include other subspecies of *Pan troglodytes,* as well as *Pan paniscus,* as it is possible that the patterns observed here are specific to *Pan troglodytes verus*. *Pongo* is the exception among the apes; all specimens studied here display a Type 1 transverse crest, similar to the majority of hominins.

The earliest hominin in our sample, *A. anamensis*, displays a Type 1 transverse crest. Haile-Selassie et al. (2004:1505) suggested that this is also the case in an *Ardipithecus kadabba* P_3 from 5.6–5.8 Ma: "The transverse crest descends from the tip of the protoconid to the metaconid, which is hardly expressed as a distinct entity". This would seem to indicate that that a Type 1 transverse crest is plesiomorphic for the hominin clade, and evolved independently in *Pongo*. However it is also possible that this state is plesiomorphic for hominids, but was lost in *Pan* and *Gorilla*. An analysis of the P_3 EDJ morphology in Miocene apes may help to shed further light on the evolutionary history of this trait. There is more

variation in the transverse crest in modern humans, where transverse crest absence is common (Type 0; 44%), and among our Neanderthal sample, in which Type 1a is relatively common (44%). In this form, the transverse crest flattens before reaching the protoconid tip. Here, it is possible that the relatively low transverse crest seen in Neanderthals is obscured due to the shape of the crown—in particular the tall, wide lingual face of the protoconid. If this were the case, then there would be no fundamental developmental difference between Types 1 and 1a; instead, the difference between the two would be due to a number of factors including the shape of the crown and the prominence of the transverse crest, which is why Type 1a may be best viewed as a subtype of Type 1. This would require further investigation, particularly concerning the developmental basis of the premolar transverse crest. Nonetheless, it appears that Type 1a, while not ubiquitous in Neanderthals, is an autapomorphy of this species.

Previous studies assessed the degree of transverse crest development at the OES (Suwa, 1990; Bailey, 2002; Irish et al., 2018). While we do not score the degree of development of the crest, presence/absence frequencies can be generated using our scoring system, allowing direct comparisons. For example, Irish et al. (2018) find all *A. africanus* and *H. naledi* specimens, as well as a third of *P. robustus* specimens, have no transverse crest. Using overlapping fossil samples, we instead find that transverse crests are ubiquitous in all three species (Table 2), suggesting that the appearance of this trait differs fundamentally between the OES and EDJ. At the OES, the premolar transverse crest is often incised by the longitudinal fissure, which runs between the two cusps along the mesiodistal axis of the tooth. A deep longitudinal fissure therefore relates to a weak transverse crest at the OES. However, a number of crown features such as the development and placement of the metaconid, and the thickness of the enamel, are likely to play a part in the development of the longitudinal fissure, and therefore influence the form of the transverse crest observed. The longitudinal fissure is an enamel feature, however, and as such has no EDJ equivalent. This means that at

445 the EDJ, the transverse crest form is less dependent on the appearance of other crown
446 features, which is advantageous when scoring multiple crown traits.

447 While hominins display relatively little variation in the form of the transverse crest, there is
448 more variation in the expression of accessory crests (Fig. 4). These crests form in the occlusal
449 basin either mesial or distal to the main transverse crest, and may connect to the protoconid
450 crest, marginal ridge, either of the main cusps, or to other accessory crests. In hominin lower
451 molars, multiple crests may form between the protoconid and metaconid; a variable feature
452 called trigonid crest patterning (Wu and Turner, 1993; Skinner et al., 2008; Bailey et al.,
453 *2*011; Martínez de Pinillos et al., 2014). Given the location of these crests, it is possible that
454 these features have similar developmental origins to the transverse crest (and accessory crests)
455 discussed here for hominin P_3. Trigonid crests are particularly common in Neanderthal lower
456 molars (Bailey, 2002, 2006), which is interesting given the high frequency of accessory crests
457 found here (and previously noted by Bailey, 2006) for the Neanderthal P_3. Martínez de
458 Pinillos et al. (2014) found substantial molar trigonid crest variation in the Sima de los
459 Huesos population at the EDJ, broadly equivalent to that of Neanderthals. Interestingly,
460 Martinón-Torres et al. (2012) reported that a high proportion of Sima de los Huesos P_3
461 specimens show distal accessory crests at the OES, as well as pronounced transverse crests,
462 when compared with modern humans. This could suggest that the same pattern may exist in
463 the Sima de los Huesos population as we have found here for Neanderthals, although this
464 would require comparing the EDJ morphologies of the two samples.

465 In the P_3, accessory crests are frequently found in large, otherwise empty, areas of the EDJ
466 occlusal basin, suggesting that the formation of accessory crests could be dependent on the
467 space available on the crown. The P_3 in Neanderthals usually display a tall protoconid crest,
468 which creates a steep, almost vertical, lingual-facing surface running from the protoconid
469 crest to the bottom of the occlusal basin of the tooth. Accessory crests are frequently present

on this face in Neanderthals. *Australopithecus africanus* and *P. robustus* far more often show accessory crests that connect to the main dentine horns, which are often particularly large, or to the transverse crest itself, which is also well developed. Moreover, Kraus and Furr (1953) suggested that accessory crests are also found in the P_3 of modern humans. Given the level of variation seen in premolar accessory crests, as well as molar trigonid crests, it seems likely that these traits are not individually determined, but are instead the result of upstream developmental processes. There are a number of ways in which this could operate. Firstly, the formation of these crests could be genetically determined, but could be only able to form where there is sufficient space for them within the occlusal basin. In this case, accessory crests could develop through some of the same developmental processes as other crests and ridges on the tooth crown (such as the protoconid crest, transverse crest, and marginal ridges in premolars), but would presumably form later in development than the main crests, which would explain their variability as they would be dependent on a number of earlier forming features. This process would be analogous to the patterning cascade model of cusp development in which cusps form where there is space for them on the crown, and are prevented from forming too closely to each other by the presence of inhibitor proteins (Polly, 1998; Jernvall, 2000; Kassai et al., 2005), with later forming cusps generally smaller and more variable than earlier forming cusps (Kondo and Townsend, 2006; Skinner and Gunz, 2010). Crests are different from cusps in that they are often found in association with other crests. In fact, the accessory cusps identified here were invariably found to be associated with other crests or cusps on the tooth crown. However, these features appear to be common in the relatively large distal fovea of *A. africanus* and *P. robustus*, as well as along the tall protoconid crest of *H. neanderthalensis*, suggesting that the available space on the crown is important.

494 Alternatively, these crests could arise as the result of biomechanical forces during the
495 development of the tooth crown. The EDJ preserves the form of the basement membrane of
496 the inner enamel epithelium, the morphology of which is determined by folding driven by
497 differential cell division in structures called enamel knots (Jernvall et al., 1994). Since the
498 accessory crests are most common on relatively tall crown structures (dentine horns of *P.*
499 *robustus,* and the protoconid crest of Neanderthals), it is possible that during the formation of
500 these structures, the process of differential cell division creates small buckles and folds in the
501 inner enamel epithelium as enamel knots do not proliferate themselves, but direct the cell
502 proliferation of adjacent regions of the developing tooth. These small buckles and folds
503 created could then go on to become the accessory ridges we see (see discussion of similar
504 features in molars in Skinner et al, 2010). It is important to note that we did not find any
505 accessory crests running parallel to the protoconid crest or the dentine horn tip; all run broadly
506 towards the crest/ridge. In this case accessory crests may be developmentally distinct from the
507 main crests and ridges of the tooth crown, which are far less variable within species.

508

509 *4.2 Marginal ridge continuity*

510 In line with other studies that have considered the mesial marginal ridge at the OES
511 (Leonard and Hegmon, 1987; Suwa et al., 1996; Ward et al., 2001; Kimbel et al., 2006;
512 Delezene and Kimbel, 2011), the morphology of the EDJ supports a transformation series
513 where a weak mesial marginal ridge, as in extant African apes and *A. anamensis*, is the
514 primitive state for hominins and a strong mesial marginal ridge, as in *A. africanus* and
515 *Paranthropus*, is derived. In *A. afarensis* Kimbel et al. (2004) highlighted 'phylogenetic
516 polymorphisms', which refers to the observation that some character states are variable in *A.*
517 *afarensis* but are fixed in the plesiomorphic condition in older hominins, like *A. anamensis*
518 and *Ardipithecus ramidus*, and fixed in the apomorphic condition in younger hominins. The

519 form of the mesial marginal ridge observed at the EDJ in this study, and at the OES in other
520 studies (Delezene and Kimbel, 2011), is congruent with such phylogenetic polymorphism.

521 Differences between our results and those from previous studies of the OES in early
522 hominins are relatively minor. For example, while Suwa (1990) found that all *A. africanus*
523 specimens show development of the lingual segment of the mesial marginal ridge, we found
524 that two *A. africanus* specimens (STW 213 and Taung) have discontinuous P_3 mesial
525 marginal ridges. However, this may be due to differences in scoring procedures, or in the
526 fossil samples used, in the two studies (the Taung P_3, for example, is unerupted and therefore
527 would not have been included in previous studies), rather than fundamental differences
528 between the EDJ and OES. The benefit of studying the EDJ is clearer in specimens that
529 display marginal ridges that are mostly well developed but interrupted; they are flattened at
530 some point along their length. This is most common in modern human and Neanderthal
531 specimens where it is likely associated with the secondary reduction of the metaconid, and
532 may reflect changing masticatory demands of the P_3 in these taxa.

533 Sakai (1967) recorded the presence of a 'trigonid notch' when looking at the EDJ of
534 modern human P_3, a feature which is equivalent to the mesial marginal ridge interruption
535 noted here. They found the feature in roughly a quarter of specimens in their sample, but did
536 not discuss any presence of a similar feature on the distal marginal ridge (although this feature
537 is less common in our sample). This trait is much clearer at the EDJ than at the OES as the
538 interruptions can be small, and are often located immediately next to the metaconid where the
539 enamel of the cusp may obscure visibility of the interruption at the OES. In fact, Sakai (1967)
540 only found the trigonid notch at the EDJ, and stated that the feature was entirely absent at the
541 OES in all specimens. In some cases, the marginal ridge interruptions are often large enough
542 that they are difficult to distinguish from the marginal ridge being entirely absent. Ultimately,
543 we need a better understanding of the developmental processes that contribute to marginal

ridge formation in order to test whether these categories represent distinct traits, or the same trait with differing levels of expression. It does appear, however, that the interruption and absence of marginal ridges seen in modern humans and Neanderthals appears to represent a secondary loss and is not homologous with the minimal expression of the mesial marginal ridge in early *Australopithecus* and extant apes. Further, the frequent presence of interruptions in the distal, as well as mesial, marginal ridges suggests that this may be distinct from the character state we find in earlier taxa.

Australopithecus africanus specimen STW 401 is the only example within this sample of an interrupted distal marginal ridge in an *Australopithecus* P_3, and is particularly interesting because the form of this trait appears to be different to that seen in later hominin specimens, and different to that often seen in the mesial marginal ridge in *Australopithecus*. In most cases, interruptions to the marginal ridge appear either side of the metaconid; the marginal ridge lowers and flattens before reaching the dentine horn. In this case, however, two portions of the distal marginal ridge overlap one another and do not meet. This appears to be a defective form of the marginal ridge in which extensions from the metaconid and protoconid crest have failed to meet and become continuous, possibly providing insights into the underlying developmental processes responsible for this structure around the occlusal basin.

4.3 Buccal grooves

The grading system used here for buccal grooves (absent, minor, marked) is comparable to those used by previous authors at the OES (Suwa, 1990) and the EDJ (Sakai, 1967), and can also be compared to studies using presence/absence scores (Wood and Uytterschaut, 1987). Our results are largely consistent with those of the OES; while there are some differences, these may be due to the samples utilized in each case, which overlap but are not identical.

568 However, it is also possible that enamel deposition affects the OES expression of buccal
569 grooves in some cases.

570 Suwa (1990) suggested that strong distal buccal grooves at the OES are a derived condition
571 for hominins; this is supported by our finding that extant apes show absent or minor EDJ
572 distal buccal grooves, while marked grooves are found in a number of *Australopithecus*
573 specimens, including one specimen of *A. anamensis*, the earliest hominin in our sample.
574 Further, ASK-VP-3/403, a P_3 of *Ar. kadabba* from 5.6–5.8 Ma, is also described as showing a
575 distinct distal buccal groove at the OES (Haile-Selassie et al., 2004, 2009). On the mesial
576 side, Suwa (1990) found that *A. afarensis* was variable, but suggested an increase in well-
577 developed OES buccal grooves in the earliest hominins compared to apes. Our results are
578 consistent with this suggestion, finding marked mesial buccal grooves in 5/6 *A. anamensis*
579 and *A. afarensis* specimens, but not in any of our extant ape specimens. The variability in *A.*
580 *afarensis* cannot be assessed here however due to the small available sample. In order to
581 further test these suggestions, the EDJ morphology of fossil apes should also be investigated.

582 *Paranthropus* is derived among hominins in showing a high level of mesial buccal groove
583 absence as noted previously (Wood and Uytterschaut, 1987; Suwa, 1990). However, we find
584 more variability in the distal buccal groove expression than Suwa (1990). In modern humans,
585 absence of mesial and distal buccal grooves is the most common form, while in Neanderthals,
586 no specimens show marked buccal grooves, and 79% (11/14) show absent distal buccal
587 grooves. However, Sakai (1967) found a higher proportion of modern human specimens with
588 buccal grooves at the EDJ, particularly on the mesial side. This could be due to a difference in
589 scoring procedure; however, it is also possible that buccal grooves are more common in the
590 Japanese sample used by Sakai (1967) than in the sample used here. This would suggest that
591 there is more variation in buccal groove expression in modern humans than is captured here,
592 and should be explored further. The majority of *H. naledi* specimens show minor buccal

grooves on the mesial and distal sides, and only one specimen (U.W. 101-144) shows an absent distal buccal groove as suggested to be typical of early *Homo* at the OES (Wood and Uytterschaut, 1987; Suwa, 1990). The *H. naledi* expression of minor EDJ mesial buccal grooves could be interpreted as derived relative to the *Australopithecus*/early *Homo* state of strongly expressed mesial buccal grooves, particularly considering the weaker expression observed in modern humans and Neanderthals.

Although there are a number of species-specific patterns in buccal groove expression as outlined above, there is also a large amount of variation. Within our sample, it appears that buccal grooves are more common in specimens showing straight protoconid crests (in occlusal view). In such a configuration, there is a more angled intersection between the protoconid crests and the mesial/distal marginal ridge, often marked by a small accessory cusp. The buccal ridge is visible as a vertical crest on the buccal surface, as well as a slight concavity next to the ridge (towards the center of the crown), which could be considered an extension of the marginal ridge on the buccal surface. In this case, the expression of buccal grooves would depend on a number of aspects of crown morphology such as the overall shape of the crown, and the configuration of major occlusal crests, which may explain the variability in this trait. This should be explored further as it would affect our understanding of the independence of buccal grooves from other crown traits.

It is also important to consider potential serial homologies (de Beer, 1971; Roth, 1994) with similar traits on other tooth positions. Based on their analysis of the EDJ of mandibular molars, Skinner et al. (2009) suggested that crest features along the entire buccal face should be considered part of the expression of the protostylid; it is possible that these crests on the molar buccal face are developmentally linked to P_3 buccal grooves (note that the name buccal 'groove' may be misleading; in most cases at the EDJ the buccal groove consists of a ridge/crest with an associated concavity). The pattern noted here in which *A. africanus*

specimens show stronger mesial buccal grooves than *P. robustus* is somewhat mirrored in Skinner et al.'s (2009) study of molar protostylid patterning. They found that *A. africanus* molars expressed a protostylid crest that extends mesially, whereas the crests in *P. robustus* specimens were mostly restricted to the area between the protoconid and hypoconid. Further, we find that STW 213 (Fig. 3, bottom image) exhibits strong buccal grooves in addition to protostylid-like crests running diagonally across the buccal face. In this case, the buccal groove and possible protostylid appear to be distinct features; however, it is interesting to note that STW 213 has the most well defined buccal grooves of any specimen within the sample. Ultimately, further investigation is required to assess the developmental basis of both of these traits.

4.4 Protoconid form

The transversely expanded dentine horn seen in ULAC 58 (Fig. 5D) may be related to the 'internally placed cusps' identified at the OES of Neanderthal molars (Tattersall and Schwartz, 1999; Bailey, 2004). Further, Martin et al. (2017) discussed the presence of 'centrally placed dentine horn tips' at the EDJ of Neanderthal and modern human molars, and the protoconid dentine horn form in the P_3 of ULAC 58 appears to fit within their typology. In fact, the molars of the ULAC 58 mandible were also included in the sample for Martin et al. (2017), where they found that the M_1 and M_3 displayed a centrally placed entoconid dentine horn. Martin et al. (2017) suggested that centrally located dentine horns were particularly common in Neanderthals. Although we did not find any Neanderthal specimens for which the protoconid was similar in form to that found in ULAC 58, we did find that the apex of the protoconid crest and the tip of the protoconid are frequently angled lingually, resulting in a more centrally located protoconid. Gómez-Robles et al. (2008) suggested that this feature is distinctive of the P_3 in Neanderthals and *H. heidelbergensis*. Unfortunately, the Mauer P_3

643 included here (and its antimere) is too worn to assess if this specimen displays the same
644 morphology.

645 Another trait discussed here, the longitudinally expanded dentine horn (Fig. 5C), also
646 relates to a feature discussed by Martin et al. (2017): twinned dentine horns. We did not find
647 this trait in any modern human or Neanderthal specimens, but it was found in several *H.*
648 *naledi* specimens, as well as a single *Pan* specimen. In some cases, the *H. naledi* P_3
649 protoconid appears simply to be expanded, rather than twinned, although it is possible that the
650 separate apices of the twinned dentine horns are too small to be visible in the scans. Martin et
651 al. (2017) also found specimens that showed 'unusually wide' dentine horns, and suggested
652 this may be a diminutive form of the twinned dentine horn trait. These traits are particularly
653 interesting since they are difficult to reconcile with the currently well-accepted patterning
654 cascade model of cuspal development (Polly, 1998; Jernvall, 2000; Kondo and Townsend,
655 2006; Skinner and Gunz, 2010), in which cusps develop iteratively across the crown, and that
656 a zone of inhibition during crown development prevents the formation of cusps in close
657 proximity to one another. Neither of the protoconid traits described here were seen on P_3
658 metaconids, although this may be due a combination of the rarity of the features, and the
659 reduced number of specimens displaying a well-developed metaconid. Although more
660 investigation is warranted before strong conclusions can be made, the twinned protoconid
661 dentine horns of *H. naledi* represent a potential autapomorphy of this species.

662

663 **5. Taxonomic implications**

664 These traits can have a bearing on the taxonomic affiliation of important specimens. For
665 example, two specimens included here, KNM-WT 8556 and W8-978, have not been
666 definitively assigned to species rank, but have been suggested to belong to *A. afarensis*
667 (Leonard and Hegmon, 1987; Suwa, 1990; Brown et al., 2001). Our results are consistent with

668 this suggestion; both specimens show fully continuous marginal ridges, a morphology that
669 first appears in *A. afarensis*, and the buccal groove forms are typical of *Australopithecus* in
670 general. However, these specimens are also roughly coeval with *Kenyanthropus platyops* and
671 *Australopithecus deyiremeda*, neither of which are included here. In fact, KNM-WT 8556 is
672 found in the same Lomekwi locality as *K. platyops*, and the P_4 and M_3 are suggested to show
673 a derived morphology, relative to *A. afarensis* (Leakey et al., 2001). Ultimately however,
674 additional fossil material of *K. platyops* is required in order to make direct comparisons to
675 mandibular specimens.

676 KNM-ER 5431 has been previously assigned to *A. afarensis* (Leonard and Hegmon, 1987),
677 while other authors have suggested the presence of *Homo*-like traits (Suwa, 1990; Wood,
678 1991). The P_3 included here, KNM-ER 5431E (Fig 1i), is found to display continuous
679 marginal ridges, which are common in a number of hominin taxa, while the buccal groove
680 form was not able to be assessed here due to poor tissue contrast in the cervical region of the
681 crown (although clear buccal grooves are evident at the OES). The transverse crest form of
682 this specimen (Type 2) is not seen in any other hominin P_3 in our sample; the crest is
683 deflected before reaching the metaconid. It is unclear whether this is an apomorphic character
684 state for a species not included in this sample, or whether this type is simply an uncommon
685 developmental variant. Since the transverse crest in this specimen is weakly expressed, this
686 may be difficult to assess from the OES, underlining the importance of trait assessment at the
687 EDJ as well as the OES.

688 STW 151 has been suggested to display a number of derived features relative to
689 Sterkfontein *A. africanus* by Moggi-Cecchi et al. (1998). However, the P_3 was not suggested
690 to show any derived *Homo* discrete traits at the OES, which is supported in our EDJ results. In
691 general, we did not find clear differences between *A. africanus* and our small sample of early
692 *Homo* specimens, except for the absence of a distal buccal groove in KNM-ER 806E, which

693 was not seen in any *Australopithecus* specimen. SKX 21204 is assigned to *Homo*, but has no
694 specific attribution (Grine, 1989). Unfortunately, the small early *Homo* sample here prevents a
695 detailed assessment of the P_3 of this specimen.

696 The Cave of Hearths mandible has not been assigned to a species, but the original
697 description and later analyses drew comparisons with the morphology seen in Neanderthals,
698 and recently Berger et al. (2017) suggested the need for comparisons with *H. naledi*. Although
699 the Cave of Hearths mandible is poorly dated, it is suggested to antedate the *H. naledi* sample
700 included here (McNabb et al., 2009; Dirks et al., 2017). We find that the discontinuous mesial
701 marginal ridge and absence of buccal grooves distinguishes the Cave of Hearths P_3 from *H.*
702 *naledi*. However, the absent buccal grooves and marginal ridge discontinuity of the P_3 are
703 common in modern humans and Neanderthals, and are also found in the Mauer P_3. This,
704 combined with the overall EDJ shape of the P_3 (Davies et al., 2019), suggests that the Cave of
705 Hearths specimen is more closely associated with modern humans, Neanderthals and
706 specimens attributed to *H. heidelbergensis*, while *H. naledi,* despite its Middle Pleistocene
707 age, displays a morphology which is more primitive. This is also supported by differences
708 between *H. naledi* and the Cave of Hearths mandible in occlusal topography of the M_2
709 (Berthaume et al., 2018) and M_1 root morphology (Kupczik et al., 2019).

710

711 **6. Conclusions**

712 We have identified several discrete P_3 traits evident at the EDJ that are variable in
713 hominoids. In some cases, the form of these traits is largely similar to that of the OES, such as
714 in buccal grooves, but in other cases, such as the transverse crest, additional morphological
715 information is evident at the EDJ that may be obscured at the OES by adjacent crown features
716 and thick enamel. A number of trends are evident in the expression of these traits. For
717 example, the transverse crest is variable in extant apes, but the majority of hominins show a

single crest connecting the protoconid to the metaconid. Absence of this crest is seen in some specimens of *P. boisei* and *H. sapiens*, while some Neanderthals show a derived form in which the crest flattens before reaching the protoconid cusp tip. The mesial marginal ridge undergoes a transformation series early in hominin evolution, from the poorly developed ancestral state seen in *A. anamensis*, through the polymorphic condition in *A. afarensis* (Kimbel et al., 2004; Delezene and Kimbel, 2011), to the well-developed marginal ridges seen in *A. africanus* and *P. robustus*. A number of modern humans and Neanderthal specimens show a secondary reduction in marginal ridge development, although this is confined to the mesial marginal ridge in Neanderthals. Buccal grooves are variable throughout hominoids, with some taxon-specific patterns, but which may be dependent on other aspects of crown morphology.

Our understanding of the development of discrete dental traits is very limited. This is important when using these traits in phylogenetic studies since the traits used should ideally be genetically independent, and care must be taken to avoid suggesting that traits that are superficially similar, but developmentally distinct, can be considered as identical (i.e., versions of the same trait) for cladistics analysis. Further, patterning cascade models to explain variation in dental form have mostly focused on the morphology of the molars. Similar homologous mechanisms presumably underlie the differences in premolar form; however, certain traits (i.e., twinned dentine horns) observed in this study are hard to explain with such a model and highlight the need for investigation of premolar form within an evolutionary-developmental framework. As shown here, studying the EDJ provides valuable insights into the development of these traits, and this will be further improved through inclusion of broader primate samples, and the study of other tooth positions at the EDJ.

742 **References**

743 Anemone, R.L., Skinner, M.M., Dirks, W., 2012. Are there two distinct types of hypocone in
744 Eocene primates? The 'pseudohypocone' of notharctines revisited. Palaeontologia
745 Electronica 15, 26A.

746 Bailey, S.E., 2002. Neandertal dental morphology: implications for modern human origins.
747 Ph.D. Dissertation, Arizona State University.

748 Bailey, S.E., 2004. A morphometric analysis of maxillary molar crowns of Middle-Late
749 Pleistocene hominins. Journal of Human Evolution 47, 183-198.

750 Bailey, S.E., 2006. Beyond shovel shaped incisors: Neandertal dental morphology in a
751 comparative context. Periodicum Biologorum 108, 253–267.

752 Bailey, S.E., Skinner, M.M., Hublin, J., 2011. What lies beneath? An evaluation of lower
753 molar trigonid crest patterns based on both dentine and enamel expression. American
754 Journal of Physical Anthropology 145, 505-518.

755 Berger, L.R., Hawks, J., Dirks, P.H., Elliott, M., Roberts, E.M., 2017. *Homo naledi* and
756 Pleistocene hominin evolution in subequatorial Africa. eLife 6, e24234.

757 Berthaume, M.A., Delezene, L.K., Kupczik, K. 2018. Dental topography and the diet of
758 *Homo naledi*. Journal of Human Evolution 118, 14-26.

759 Beynon, A.D., Wood, B.A., 1986. Variations in enamel thickness and structure in East
760 African hominids. American Journal of Physical Anthropology 70, 177-193.

761 Braga, J., Thackeray, J.F., Subsol, G., Kahn, J.L., Maret, D., Treil, J. and Beck, A., 2010. The
762 enamel–dentine junction in the postcanine dentition of *Australopithecus africanus*:
763 intra-individual metameric and antimeric variation. Journal of Anatomy 216, 62-79.

764 Brown, B., Brown, F.H., Walker, A., 2001. New hominids from the Lake Turkana Basin,
765 Kenya. Journal of Human Evolution 41, 29-44.

766 Brunet, M., Guy, F., Pilbeam, D., Mackaye, H.T., Likius, A., Ahounta, D., Beauvilain, A.,
767 Blondel, C., Bocherens, H., Boisserie, J. De Bonis, L., Coppens, Y., Dejax, J., Denys, C.,
768 Duringer, P., Eisenmann, V., Fanone, G., Fronty, P., Geraads, D., Lehmann, T., Lihoreau,
769 F., Louchart, A., Mahamat, A., Merceron, G., Mouchelin, G., Otero, O., Campomanes,
770 P.P., De Leon, M.P., Rage, J., Sapanet, M., Schuster, M., Sudre, J., Tassy, P., Valentin, X.,
771 Vignaud, P., Viriot, L., Zazzo, A., Zollikofer, C., 2002. A new hominid from the Upper
772 Miocene of Chad, Central Africa. Nature 418, 145-151.

773 Burnett, S.E., Irish, J.D., Fong, M.R., 2013. Wear's the problem? Examining the effect of
774 dental wear on studies of crown morphology. In: Scott, G.R., Irish, J.D. (Eds.),
775 Anthropological Perspectives on Tooth Morphology: Genetics, Evolution, Variation.
776 Cambridge University Press, Cambridge, pp. 535-554.

777 Corruccini, R.S., 1987. The dentinoenamel junction in primates. International Journal of
778 Primatology 8, 99-114

779 de Beer, S.G., 1971. Homology, an Unsolved Problem. Oxford University Press, London.

780 Delezene, L.K., 2015. Modularity of the anthropoid dentition: Implications for the evolution
781 of the hominin canine honing complex. Journal of Human Evolution 86, 1-12.

782 Delezene, L.K., Kimbel, W.H., 2011. Evolution of the mandibular third premolar crown in
783 early *Australopithecus*. Journal of Human Evolution 60, 711-730.

784 Dempsey, P.A. and Townsend, G.C., 2001. Genetic and environmental contributions to
785 variation in human tooth size. Heredity 86, 685-693.

786 Dirks, P.H., Roberts, E.M., Hilbert-Wolf, H., Kramers, J.D., Hawks, J., Dosseto, A., Duval,
787 M., Elliott, M., Evans, M., Grün, R., Hellstrom, J., 2017. The age of *Homo naledi* and
788 associated sediments in the Rising Star Cave, South Africa. eLife 6, e24231.

789 Gómez-Robles, A., Martinón-Torres, M., Bermúdez de Castro, J.M., Prado, L., Sarmiento, S.,
790 Arsuaga, J.L., 2008. Geometric morphometric analysis of the crown morphology of the
791 lower first premolar of hominins, with special attention to Pleistocene *Homo*. Journal of
792 Human Evolution 55*,* 627-638.

793 Greenfield, L.O., 1990. Canine "honing" in *Australopithecus afarensis*. American Journal of
794 Physical Anthropology 82, 135-143.

795 Greenfield, L.O., Washburn, A., 1992. Polymorphic aspects of male anthropoid honing
796 premolars. American Journal of Physical Anthropology 87, 173-186.

797 Grine, F.E., 1989. New hominid fossils from the Swartkrans Formation (1979–1986
798 excavations): craniodental specimens. American Journal of Physical Anthropology 79,
799 409-449.

800 Grine, F.E., Sponheimer, M., Ungar, P.S., Lee-Thorp, J., Teaford, M.F., 2012. Dental
801 microwear and stable isotopes inform the paleoecology of extinct hominins. American
802 Journal of Physical Anthropology 148, 285-317.

803 Guy, F., Lazzari, V., Gilissen, E., Thiery, G., 2015. To what extent is primate second molar
804 enamel occlusal morphology shaped by the enamel-dentine junction? PLoS One 10,
805 e0138802.

806 Haile-Selassie, Y., Suwa, G., White, T.D., 2009. Hominidae. In: Haile-Selassie Y.,
807 WoldeGabriel G., (Eds.), *Ardipithecus kadabba*. Evidence from the Late Miocene of
808 Africa. University of California Press, Berkeley and Los Angeles, pp.159-236.

809 Haile-Selassie, Y., Suwa, G., White, T.D. 2004. Late Miocene teeth from Middle Awash,
810 Ethiopia, and early hominid dental evolution. Science 303, 1503-1505.

811 Hlusko, L.J., Mahaney, M.C. 2003. Genetic contributions to expression of the baboon
812 cingular remnant. Archives of Oral Biology 48, 663-672.

813 Irish, J.D., Guatelli-Steinberg, D., 2003. Ancient teeth and modern human origins: an
814 expanded comparison of African Plio-Pleistocene and recent world dental samples. Journal
815 of Human Evolution 45, 113-144.

816 Irish, J.D., Bailey, S.E., Guatelli-Steinberg, D., Delezene, L.K., Berger, L.R., 2018. Ancient
817 teeth, phenetic affinities, and African hominins: Another look at where *Homo naledi* fits in.
818 Journal of Human Evolution 122, 108-123

819 Jernvall, J., 2000. Linking development with generation of novelty in mammalian teeth.
820 Proceedings of the National Academy of Sciences USA 97, 2641-2645.

821 Jernvall, J., Kettunen, P., Karavanova, I., Martin, L.B., Thesleff, I., 1994. Evidence for the
822 role of the enamel knot as a control center in mammalian tooth cusp formation: non-
823 dividing cells express growth stimulating Fgf-4 gene. The International Journal of
824 Developmental Biology 38*,* 463-469.

825 Kassai, Y., Munne, P., Hotta, Y., Penttilä, E., Kavanagh, K., Ohbayashi, N., Takada, S.,
826 Thesleff, I., Jernvall, J., Itoh, N., 2005. Regulation of mammalian tooth cusp patterning by
827 ectodin. Science 309, 2067-2070.

828 Kettunen, P., Thesleff, I. 1998. Expression and function of FGFs-4, -8, and -9 suggest
829 functional redundancy and repetitive use as epithelial signals during tooth morphogenesis.
830 Developmental Dynamics 211, 256-268.

831 Kimbel, W.H., Rak, Y., Johanson, D.C., 2004. The Skull of *Australopithecus afarensis*.
832 Oxford University Press, New York.

833 Kimbel, W.H., Lockwood, C.A., Ward, C.V., Leakey, M.G., Rak, Y., Johanson, D.C., 2006.
834 Was *Australopithecus anamensis* ancestral to *A. afarensis*? A case of anagenesis in the
835 hominin fossil record. Journal of Human Evolution 51, 134-152.

836 Kondo, S., Townsend, G.C., 2006. Associations between Carabelli trait and cusp areas in
837 human permanent maxillary first molars. American Journal of Physical Anthropology 129,
838 196-203.

839 Korenhof, C.A.W., 1960. Morphogenetical Aspects of the Human Upper Molar.
840 Uitgeversmaatschappij Neerlandia, Utrecht.

841 Kraus, B.S., Furr, M.L., 1953. Lower first premolars. Part I. A definition and classification of
842 discrete morphologic traits. Journal of Dental Research 32, 554-564.

843 Krenn, V.A., Fornai, C., Wurm, L., Bookstein, F.L., Haeusler, M., Weber, G.W., 2019.
844 Variation of 3D outer and inner crown morphology in modern human mandibular
845 premolars. American Journal of Physical Anthropology 168, 646-663.

846 Kupczik, K., Delezene, L.K., Skinner, M.M. 2019. Mandibular molar root and pulp cavity
847 morphology in *Homo naledi* and other Plio-Pleistocene hominins. Journal of Human
848 Evolution 130, 83-95.

849 Leakey, M.G., Spoor, F., Brown, F.H., Gathogo, P.N., Kiarie, C., Leakey, L.N., McDougall,
850 I., 2001. New hominin genus from eastern Africa shows diverse middle Pliocene lineages.
851 Nature 410, 433-440.

852 Lee-Thorp, J.A., Sponheimer, M., van der Merwe, N.J., 2003. What do stable isotopes tell us
853 about hominid dietary and ecological niches in the Pliocene? International Journal of
854 Osteoarchaeology 13, 104-113.

855 Leonard, W.R., Hegmon, M., 1987. Evolution of P_3 morphology in *Australopithecus*
856 *afarensis*. American Journal of Physical Anthropology 73, 41-63

857 Liao, W., Xing, S., Li, D., Martinón-Torres, M., Wu, X., Soligo, C., de Castro, J.M.B., Wang,
858 W., Liu, W., 2019. Mosaic dental morphology in a terminal Pleistocene hominin from
859 Dushan Cave in southern China. Scientific Reports 9, 2347.

860 Liu, W., Schepartz, L.A., Xing, S., Miller-Antonio, S., Wu, X., Trinkaus, E., Martinón-
861 Torres, M., 2013. Late middle pleistocene hominin teeth from Panxian Dadong, South
862 China. Journal of Human Evolution 64, 337-355.

863 Macho, G.A., Thackeray, J.F., 1992. Computed tomography and enamel thickness of
864 maxillary molars of Plio-Pleistocene hominids from Sterkfontein, Swartkrans, and
865 Kromdraai (South Africa): An exploratory study. American Journal of Physical
866 Anthropology 89, 133-143.

867 Martin, R.M., Hublin, J.-J., Gunz, P., Skinner, M.M., 2017. The morphology of the enamel–
868 dentine junction in Neanderthal molars: Gross morphology, non-metric traits, and temporal
869 trends. Journal of Human Evolution 103, 20-44.

870 Martínez de Pinillos, M., Martinón-Torres, M., Skinner, M.M., Arsuaga, J.L., Gracia-Téllez,
871 A., Martínez, I., Martín-Francés, L., Bermúdez de Castro, J.M., 2014. Trigonid crests
872 expression in Atapuerca-Sima de los Huesos lower molars: Internal and external
873 morphological expression and evolutionary inferences. Comptes Rendus Palevol 13, 205-
874 221.

875 Martinón-Torres, M., Bermúdez de Castro, J.M., Gómez-Robles, A., Prado-Simón, L.,
876 Arsuaga, J.L., 2012. Morphological description and comparison of the dental remains from
877 Atapuerca-Sima de los Huesos site (Spain). Journal of Human Evolution 62, 7-58.

878 Martinón-Torres, M., de Pinillos, M.M., Skinner, M.M., Martín-Francés, L., Gracia-Téllez,
879 A., Martínez, I., Arsuaga, J.L., Bermúdez de Castro, J.M., 2014. Talonid crests expression
880 at the enamel–dentine junction of hominin lower permanent and deciduous molars.
881 Comptes Rendus Palevol 13, 223-234.

882 McNabb, J., Sinclair, A., Wadley, L., Maguire, J., Latham, A., Herries, A., Ogola, C., Curnoe,
883 D., Underhill, D. 2009. The Cave of Hearths: Makapan Middle Pleistocene Research
884 Project: Field Research by Anthony Sinclair and Patrick Quinney, 1996-2001.
885 Archaeopress, Oxford.

886 Moggi-Cecchi, J., Tobias, P.V., Beynon, A.D., 1998. The mixed dentition and associated
887 skull fragments of a juvenile fossil hominid from Sterkfontein, South Africa. American
888 Journal of Physical Anthropology 106, 425-465.

889 Morita, W., Yano, W., Nagaoka, T., Abe, M., Ohshima, H., Nakatsukasa, M. 2014. Patterns
890 of morphological variation in enamel–dentin junction and outer enamel surface of human
891 molars. Journal of Anatomy 224, 669-680.

892 Nager, G., 1960. Der vergleich zwischen dem räumlichen verhalten des dentin-kronenreliefs
893 und dem schmelzrelief der zahnkrone. Cells Tissues Organs 42, 226-250.

894 Ortiz, A., Skinner, M.M., Bailey, S.E., Hublin, J.-J., 2012. Carabelli's trait revisited: An
895 examination of mesiolingual features at the enamel–dentine junction and enamel surface of
896 *Pan* and *Homo sapiens* upper molars. Journal of Human Evolution 63, 586-596.

897 Polly, P.D., 1998. Variability, selection, and constraints: development and evolution in
898 viverravid (Carnivora, Mammalia) molar morphology. Paleobiology 24, 409-429.

899 Richards, M.P., Pettitt, P.B., Stiner, M.C., Trinkaus, E., 2001. Stable isotope evidence for
900 increasing dietary breadth in the European mid-Upper Paleolithic. Proceedings of the
901 National Academy of Sciences USA 98, 6528-6532.

902 Robinson, J.T., 1956. The Dentition of the Australopithecinae. Transvaal Museum, Pretoria.

903 Roth, V.L., 1994. Within and Between Organisms: Replicators, Lineages, and Homologues.
904 In: Hall, B.K., (Ed.), Homology: The Hierarchical Basis of Comparative Biology.
905 Academic Press, San Diego, pp 301–337

906 Sakai, T., 1967. Morphologic study of the dentinoenamel junction of the mandibular first
907 premolar. Journal Dental Research 46, 927-932

908 Schulze, M.A., Pearce, J.A., 1994. A morphology-based filter structure for edge-enhancing
909 smoothing. In: Proceedings of the 1994 IEEE International Conference on Image
910 Processing, pp. 530–534

911 Skinner, M.M., 2008. Enamel-dentine junction morphology of extant hominoid and fossil
912 hominin mandibular molars. Ph.D. Dissertation, George Washington University.

913 Skinner, M.M., Gunz, P., 2010. The presence of accessory cusps in chimpanzee lower molars
914 is consistent with a patterning cascade model of development. Journal of Anatomy 217,
915 245-253.

916 Skinner, M.M., Wood, B.A., Boesch, C., Olejniczak, A.J., Rosas, A., Smith, T.M., Hublin,
917 J.J., 2008. Dental trait expression at the enamel-dentine junction of lower molars in extant
918 and fossil hominoids. Journal of Human Evolution 54, 173-186.

919 Skinner, M.M., Wood, B.A., Hublin, J.-J., 2009. Protostylid expression at the enamel-dentine
920 junction and enamel surface of mandibular molars of *Paranthropus robustus* and
921 *Australopithecus africanus*. Journal of Human Evolution *56*, 76-85.

922 Skinner, M.M., Evans, A., Smith, T., Jernvall, J., Tafforeau, P., Kupczik, K., Olejniczak, A.J.,
923 Rosas, A., Radovčić, J., Thackeray, J.F., Toussaint, M., Hublin, J.-J., 2010. Brief
924 communication: Contributions of enamel-dentine junction shape and enamel deposition to
925 primate molar crown complexity. American Journal of Physical Anthropology 142, 157-
926 163.

927 Smith, T.M., Olejniczak, A.J., Zermeno, J.P., Tafforeau, P., Skinner, M.M., Hoffmann, A.,
928 Radovčić, J., Toussaint, M., Kruszynski, R., and Menter, C., 2012. Variation in enamel
929 thickness within the genus *Homo*. Journal of Human Evolution 62, 395-411.

930 Sponheimer, M., Lee-Thorp, J.A., 1999. Isotopic evidence for the diet of an early hominid,
931 *Australopithecus africanus*. Science 283, 368-370.

932 Suwa, G., 1988. Evolution of the "robust" australopithecines in the Omo succession: evidence
933 from mandibular premolar morphology. In: Grine, F.E. (Ed.), Evolutionary History of the
934 "Robust" Australopithecines. Aldine de Gruyter, New York, pp. 199-222.

935 Suwa, G., 1990. A comparative analysis of hominid dental remains from the Shungura and
936 Usno Formations, Omo valley, Ethiopia. Ph.D. Dissertation, University of California,
937 Berkeley.

938 Suwa, G., White, T.D., Howell, F.C., 1996. Mandibular postcanine dentition from the
939 Shungura Formation, Ethiopia: crown morphology, taxonomic allocations, and Plio-
940 Pleistocene hominid evolution. American Journal of Physical Anthropology 101, 247-282.

941 Suwa, G., Kono, R.T., Simpson, S.W., Asfaw, B., Lovejoy, C.O., White, T.D., 2009.
942 Paleobiological implications of the *Ardipithecus ramidus* dentition. Science 326, 69-99.

943 Tattersall, I, Schwartz, J.H., 1999. Hominids and hybrids: The place of Neanderthals in
944 human evolution. Proceedings of the National Academy of Sciences USA 96, 7117-7119.

945 Townsend, G.C., Martin, N.G. 1992. Fitting genetic models to Carabelli trait data in South
946 Australian twins. Journal of Dental Research 71, 403-409.

947 Visualization Sciences Group, 2010. AVIZO, Version 6.3. Visualization Sciences Group,
948 Bordeaux.

949 Walker, A., 1984. Mechanisms of honing in the male baboon canine. American Journal of
950 Physical Anthropology 65, 47-60.

951 Walker, A., Hoeck, H.N., Perez, L., 1978. Microwear of mammalian teeth as an indicator of
952 diet. Science 201, 908-910.

953 Ward, C.V., Leakey, M.G., Walker, A., 2001. Morphology of *Australopithecus anamensis*
954 from Kanapoi and Allia Bay, Kenya. Journal of Human Evolution 41, 255-368.

955 Wollny, G., Kellman, P., Ledesma-Carbayo, M.J., Skinner, M.M., Hublin, J.-J., Hierl, T.,
956 2013. MIA-A free and open source software for gray scale medical image analysis. Source
957 Code for Biology and Medicine 8, 20.

958 Wood, B.A., 1991. Koobi Fora Research Project: Volume 4. Hominid Cranial Remains.
959 Clarendon Press, Oxford.

960 Wood, B.A., Abbott, S.A., 1983. Analysis of the dental morphology of Plio-Pleistocene
961 hominids. I. Mandibular molars: crown area measurements and morphological traits.
962 Journal of Anatomy 136, 197-219.

963 Wood, B.A., Uytterschaut, H., 1987. Analysis of the dental morphology of Plio-Pleistocene
964 hominids. III. Mandibular premolar crowns. Journal of Anatomy 154, 121-156.

965 Wood, B.A., Abbott, S.A., Graham, S.H., 1983. Analysis of the dental morphology of Plio-
966 Pleistocene hominids. II. Mandibular molars – study of cusp areas, fissure pattern and
967 cross sectional shape of the crown. Journal of Anatomy 137, 287-314.

968 Wu, L., Turner II, C.G., 1993. Variation in the frequency and form of the lower permanent
969 molar middle trigonid crest. American Journal of Physical Anthropology 91, 245-248.

970 Zanolli, C., 2015. Molar crown inner structural organization in Javanese *Homo erectus*.
971 American Journal of Physical Anthropology 156, 148-157.

972 Zanolli, C., Mazurier, A., 2013. Endostructural characterization of the *H. heidelbergensis*
973 dental remains from the early Middle Pleistocene site of Tighenif, Algeria. Comptes
974 Rendus Palevol 12, 293-304.

975 Zanolli, C., Pan, L., Dumoncel, J., Kullmer, O., Kundrát, M., Liu, W., Macchiarelli, R.,
976 Mancini, L., Schrenk, F., Tuniz, C., 2018. Inner tooth morphology of *Homo erectus* from

977 Zhoukoudian. New evidence from an old collection housed at Uppsala University, Sweden.
978 Journal of Human Evolution 116, 1-13.

979

980 **Figure captions**

981

982 **Figure 1.** Transverse crest variation. Illustration of the 5 main transverse crest forms seen in
983 hominoid P_3, as well as examples of each type. Schematic diagrams represent a left sided
984 tooth in occlusal view. Filled black circle indicates the protoconid, dashed circle indicates the
985 metaconid (or equivalent point on the crown, when a metaconid is not present). Example
986 EDJs are chosen to illustrate the range of variation encompassed within each type (some are
987 reversed such that all specimens appear left-sided): a) ULAC 797 (*H. sapiens*, reversed); b)
988 ULAC 171 (*H. sapiens*); c) SK 100 (*P. robustus*, reversed); d) ZMB 38607 (*Pongo*, reversed);
989 e) KRP 51 (*H. neanderthalensis*, reversed); f) KRP D33 (*H. neanderthalensis*); g) KRP D114
990 (*H. neanderthalensis*); h) ZMB 7826 (*Hylobates*); i) KNM-ER 5431E (Hominidae gen. et sp.
991 indet.); j) ZMB 31435 (*Gorilla*, reversed); k) MPITC 11776 (*Pan*); l) ZMB 7814 (*Hylobates*).
992 Abbreviations: B = buccal; L = lingual; M = mesial; D = distal.

993

994 **Figure 2.** Marginal ridge continuity. Specimens are presented in lingual view at the OES
995 (left) and EDJ (right), illustrating continuous and three types of discontinuous marginal ridges
996 (indicated by white arrows). Specimens used, top to bottom: DNH 107 (*P. robustus*), KRP 54
997 (*H. neanderthalensis*), ULAC 801 (*H. sapiens*), and ULAC 806 (*H. sapiens*). Abbreviations:
998 M = mesial; D = distal.

999 **Figure 3.** Buccal groove variation. Three specimens in buccal view at the OES (left) and EDJ
1000 (right), illustrating the range in buccal groove expression, and the scoring system used. Buccal

grooves are indicated by white arrows. Examples used are those which display the same buccal groove score mesially and distally. Top: KRP 54 (*H. neanderthalensis*). Middle: UW101 889 (*H. naledi*). Bottom: STW 213 (*A. africanus*, reversed). Abbreviations: M = mesial; D = distal.

Figure 4. Accessory crest examples. A selection of P_3 specimens displaying accessory crests, marked with white arrows. Top row in oblique view, bottom row in lingual view. The images of SK 100, DNH 46 and Combe-Grenal I have been flipped such that all specimens appear left sided. Abbreviations: B = buccal; L = lingual; M = mesial; D = distal.

Figure 5. Protoconid variation. Four specimens showing variation in protoconid form are displayed. A) 'Standard' simple conic dentine horn in SK 100 (*P. robustus*). B) Flat ridge in ULAC 790 (*H. sapiens*, image flipped). C) 'Double' dentine in UW101 377 (*H. naledi*). D) Transversely expanded dentine horn in ULAC 58 (*H. sapiens*). A–C presented as right sided in lingual view, D left sided in distal view. Abbreviations: B = buccal; L = lingual; M = mesial; D = distal.

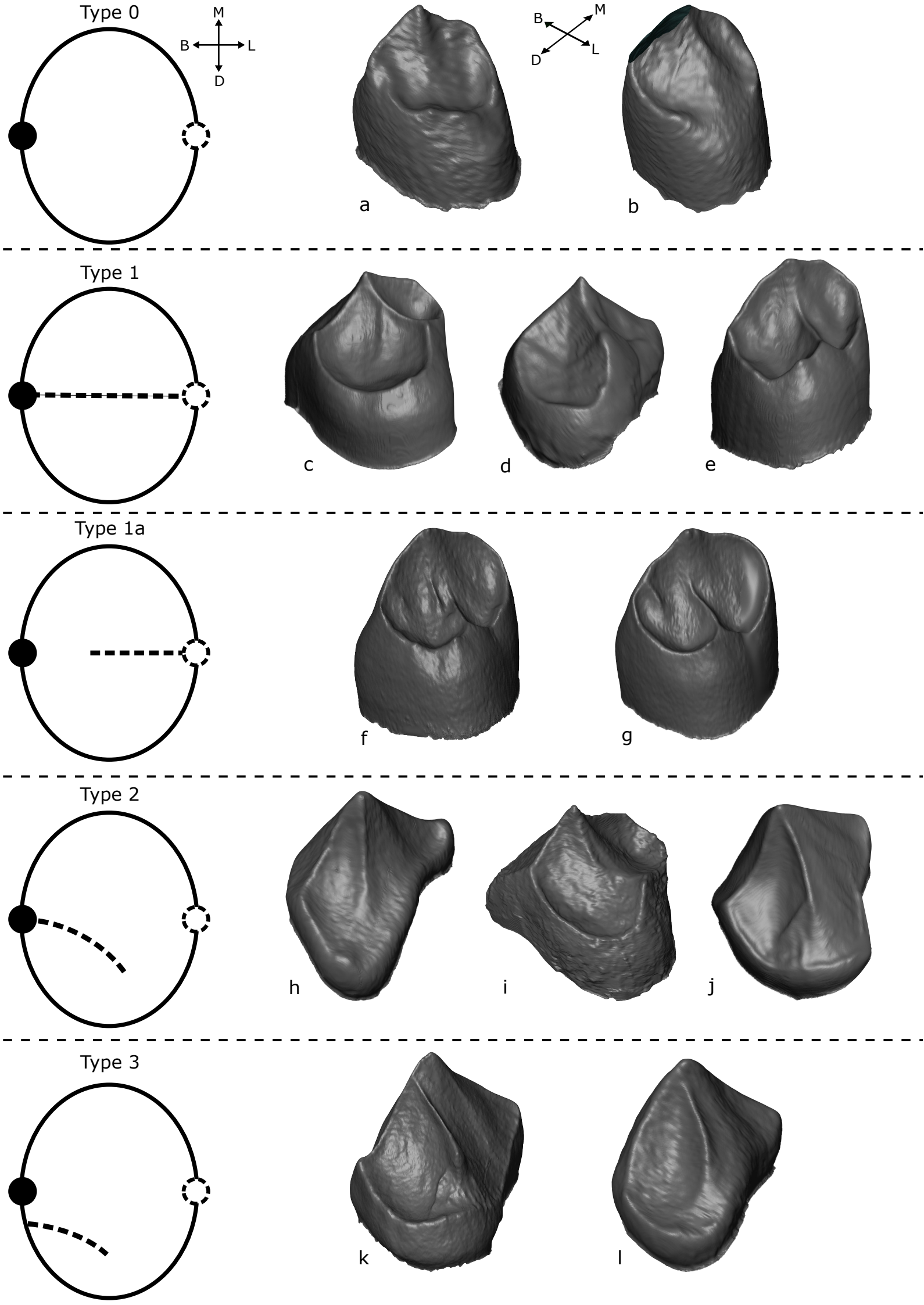
Type 0
M
B
L
D
a
B
M
D
L
b
Type 1
c
d
e
Type 1a
f
g
Type 2
h
i
j
Type 3
k
l

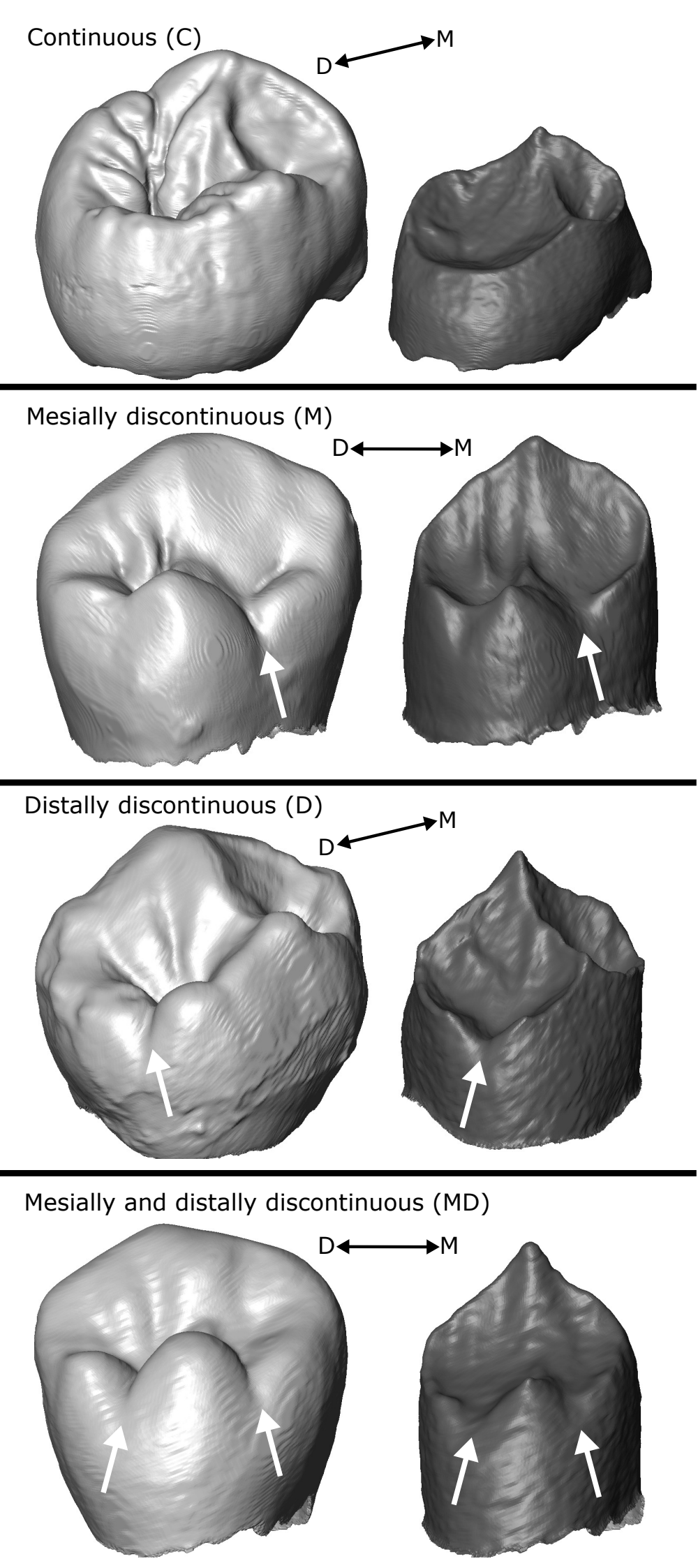
Continuous (C)
D
M
Mesially discontinuous (M)
D
M
Distally discontinuous (D)
D
M
Mesially and distally discontinuous (MD)
D
M

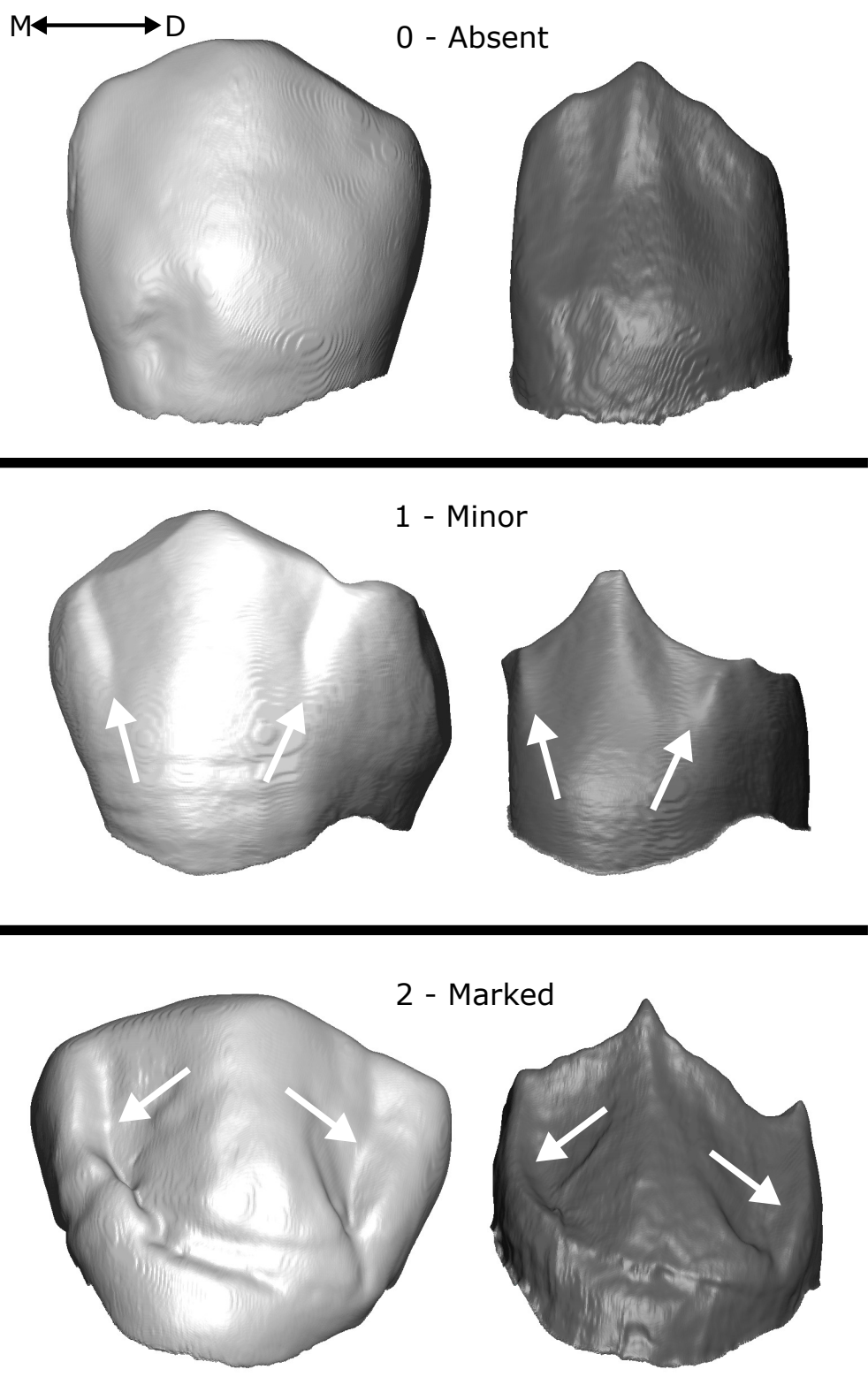
M
D
0 - Absent
1 - Minor
2 - Marked

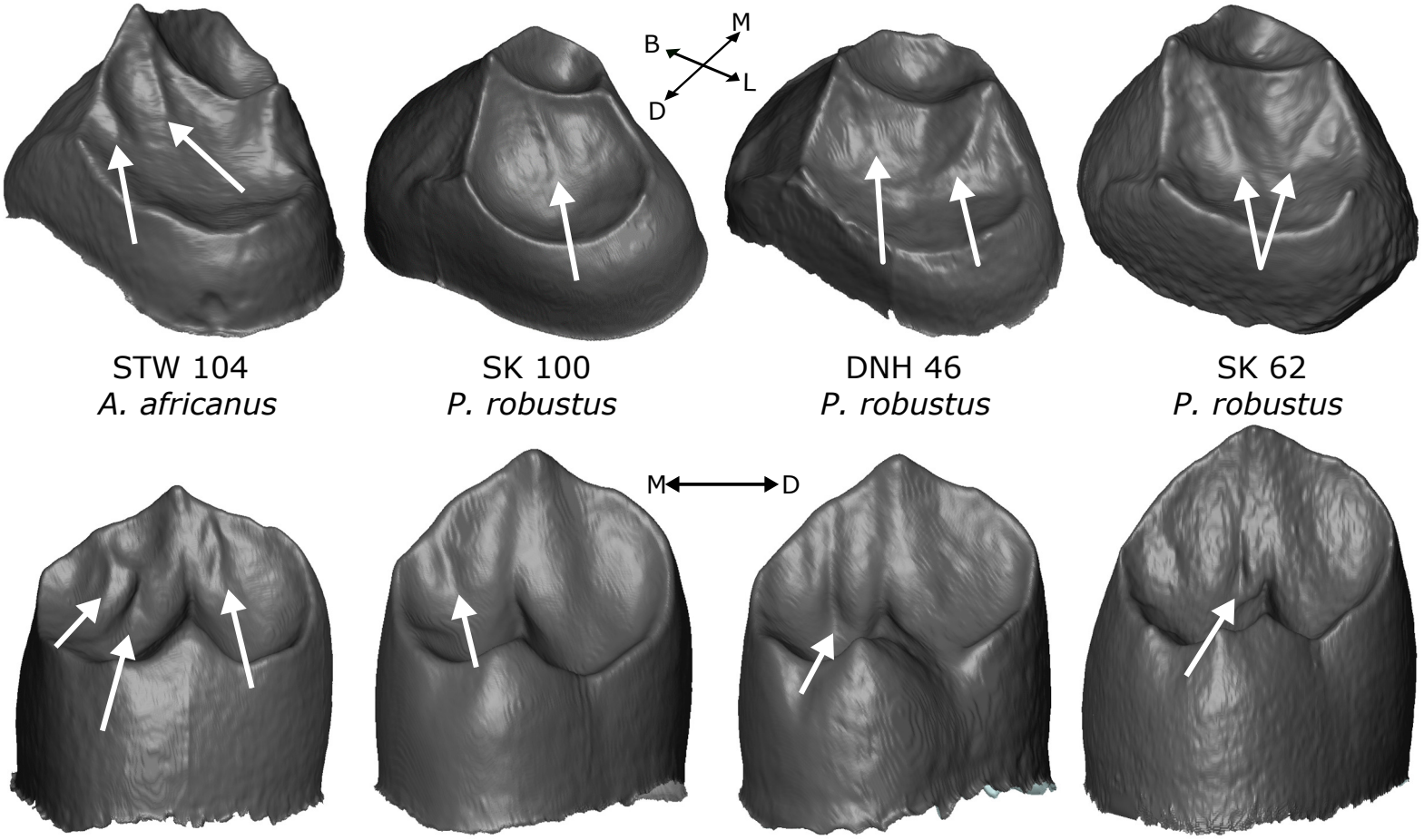

STW 104
A. africanus

SK 100
P. robustus

DNH 46
P. robustus

SK 62
P. robustus

Combe-Grenal I
H. neanderthalensis

KRP 52
H. neanderthalensis

KRP 54
H. neanderthalensis

KRP D33
H. neanderthalensis

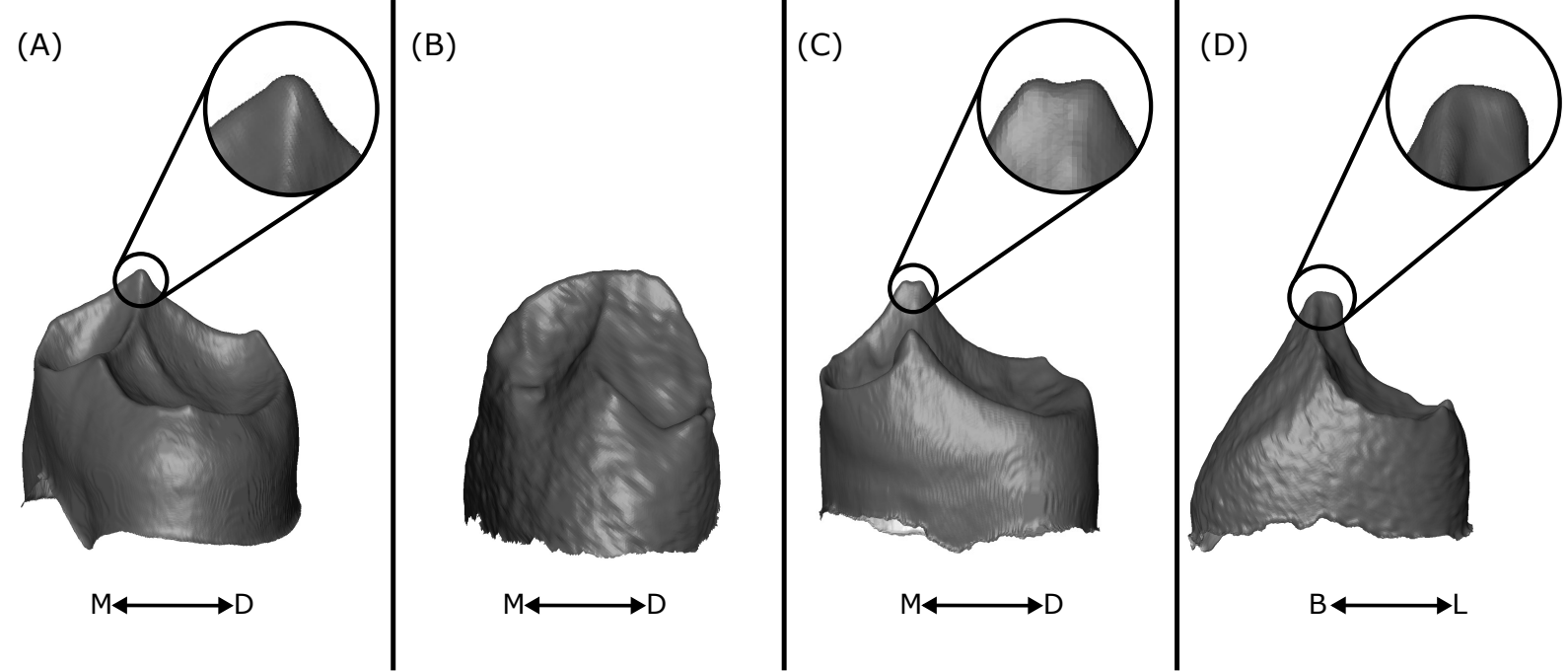
(A)
M
D
(B)
M
D
(C)
M
D
(D)
B
L

Table 1

P_3 study sample summary. The extant and fossil taxa included in the sample are listed, along with their locality, and the sample size for each of the discrete traits scored. Full specimen list can be found in SOM Table S1.[a]

Taxon	Locality	Transverse crest	Marginal ridge	Buccal grooves
Hylobates	South East Asia (*Hy. muelleri* and *Hy. agilis*)	4	–	4
Pongo	Borneo; Sumatra (*Po. pygmaeus* and *Po. abelii*)	6	–	6
Gorilla	Cameroon; Congo (*G. gorilla*)	5	–	5
Pan	Côte d'Ivoire (*Pa. troglodytes verus*)	5	–	5
A. anamensis	Kanapoi, Kenya	2	3	3
A. afarensis	Hadar and Omo, Ethiopia	4	3	3
A. africanus	Sterkfontein and Taung, South Africa	7	12	13
P. robustus	Drimolen and Swartkrans, South Africa	7	9	11
P. boisei	Koobi Fora and West Turkana, Kenya; Omo, Ethiopia	4	3	3
Homo sp.	Koobi Fora, Kenya; Swartkrans, South Africa	1	1	2
H. naledi	Rising Star cave system, South Africa	4	5	7
H. heidelbergensis	Mauer, Germany	0	1	1
H. neanderthalensis	Combe Grenal, France; Krapina, Croatia; Scladina, Belgium	9	13	14
H. sapiens	Qafzeh, Israel; Anatomical collection, various localities	9	14	14

[a] Specimens not included in these taxon groups are Cave of Hearths, KNM-ER 5431E, KNM-WT 8556, Mauer, STW 151 and W8-978.

Table 2

Transverse crest (TC) variation by taxon. The percentage of specimens displaying each transverse crest type is shown for each taxon (sample sizes in parentheses). See main text and Figure 2 for full details of the typology. For results by specimen, see SOM Table S1.[a]

Taxon (*n*)	TC type (%)				
	0	1	1a	2	3
Hylobates (4)	0	0	0	50	50
Pongo (6)	0	100	0	0	0
Gorilla (5)	0	0	0	100	0
Pan (5)	0	0	0	20	80
A. anamensis (2)	0	100	0	0	0
A. afarensis (4)	0	100	0	0	0
A. africanus (7)	0	100	0	0	0
P. robustus (7)	0	100	0	0	0
P. boisei (4)	50	50	0	0	0
Homo sp. (1)	0	100	0	0	0
H. naledi (4)	0	100	0	0	0
H. neanderthalensis (9)	0	56	44	0	0
H. sapiens (9)	44	56	0	0	0
Extant ape total (20)	0	30	0	40	30
Hominin total (51)	12	78	8	2	0

[a] Specimens which could not be assigned to taxon groups (transverse crest type in parentheses): Cave of Hearths (1), KNM-ER 5431E (2), KNM-WT 8556 (1), STW 151 (1).

Table 3

Marginal ridge (MR) variation. The percentage of specimens displaying each marginal ridge type is shown for each taxon (sample sizes in parentheses). See main text and Figure 3 for full details of the typology. For results by specimen, see SOM Table S1.

Taxon (*n*)	MR type (%)			
	C	M	D	MD
A. anamensis (3)	0	100	0	0
A. afarensis (3)	33	67	0	0
A. africanus (12)	75	17	8	0
P. robustus (9)	100	0	0	0
P. boisei (3)	100	0	0	0
Homo sp. (1)	100	0	0	0
H. naledi (5)	100	0	0	0
H. heidelbergensis (1)	0	0	0	100
H. neanderthalensis (13)	69	31	0	0
H. sapiens (14)	50	14	7	29
Hominin total (69)	70	20	3	7

Abbreviations: C = continuous; M = mesially discontinuous; D = distally discontinuous; MD = mesially and distally discontinuous

[a] Specimens which could not be assigned to taxon groups (marginal ridge type in parentheses): Cave of Hearths (M), KNM-ER 5431E (C), KNM-WT 8556 (C), STW 151 (C), W8-978 (C).

Table 4

Buccal groove variation. The percentage of specimens displaying each mesial and distal buccal groove type is shown for each taxon (sample sizes in parentheses). See main text and Figure 4 for full details of the typology. For results by specimen, see SOM Table S1.[a]

Taxon (*n*)	MBG type (%)[b]			DBG type (%)[b]		
	0	1	2	0	1	2
Hylobates (4)	75	25	0	100	0	0
Pongo (6)	100	0	0	100	0	0
Gorilla (5)	60	40	0	0	100	0
Pan (5)	40	60	0	0	100	0
A. anamensis (3)	0	0	100	0	67	33
A. afarensis (3)	0	33	67	0	33	67
A. africanus (13)	0	15	85	0	69	31
P. robustus (11)	91	9	0	18	64	18
P. boisei (3)	67	0	33	33	33	33
Homo sp. (2)	0	0	100	50	50	0
H. naledi (7)	14	86	0	14	86	0
H. heidelbergensis (1)	100	0	0	100	0	0
H. neanderthalensis (14)	43	57	0	79	21	0
H. sapiens (14)	93	7	0	86	14	0
Extant ape total (20)	70	30	0	50	50	0
Hominin total (75)	45	25	29	40	45	15

Abbreviations: MBG = mesial buccal groove; DBG = distal buccal groove.

[a] Specimens which could not be assigned to taxon groups (buccal groove types in parentheses in the form MBG:DBG): Cave of Hearths (0:0), KNM-WT 8556 (2:1), STW 151 (2:2), W8-978 (2:1).

[b] MBG and DBG states: 0 = absent; 1 = minor; 2 = marked.

Supplementary Online Material (SOM)

Endostructural morphology in hominoid mandibular third premolars: Discrete traits at the enamel-dentine junction

Thomas W. Davies[a,b,*], Lucas K. Delezene[c], Philipp Gunz[b], Jean-Jacques Hublin[b], Matthew M. Skinner[a,b]

[a] *School of Anthropology and Conservation, University of Kent, Canterbury, CT2 7NZ, UK*

[b] *Department of Human Evolution, Max Planck Institute for Evolutionary Anthropology, Deutscher Platz 6, 04103 Leipzig, Germany*

[c]*Department of Anthropology, University of Arkansas, Fayetteville, Arkansas, 72701 USA*

*Corresponding author.

E-mail address: thomas_davies@eva.mpg.de (T.W. Davies)

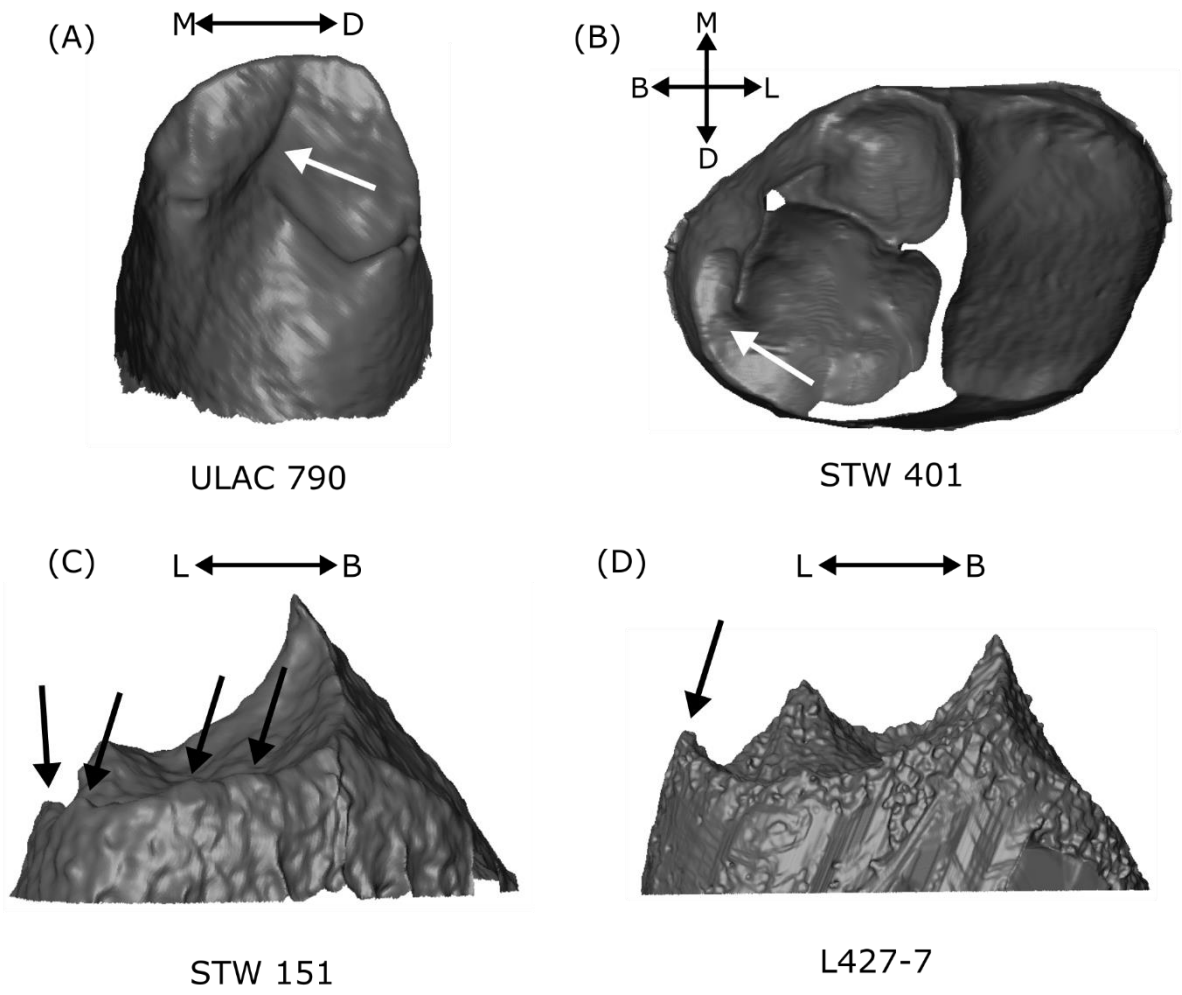

SOM Figure S1. EDJ surface for selected specimens discussed in the main text. A) ULAC 790 (reversed) in lingual view, arrow indicates transverse crest. B) STW 401 in occlusal view, arrow indicates discontinuous distal marginal ridge. C) STW 151 in distal view, arrows indicate possible accessory cusps. D) L427-7 in distal view, arrow indicates accessory cusp.

SOM Table S1. Detailed study sample, including which analyses each specimen is included in.

Specimen	Side	Site/Origin	Taxonomy	Source	Position basis[a]	Position source	TC	MR	MBG	DBG	Recon ?
ZMB 7814	L	Borneo	*Hylobates muelleri*	ZMB records	1	ZMB records	3	—	0	0	—
ZMB 7826	L	Borneo	*Hylobates muelleri*	ZMB records	1	ZMB records	2	—	1	0	—
ZMB 7828	L	Borneo	*Hylobates muelleri*	ZMB records	1	ZMB records	3	—	0	0	—
ZMB 85368	L	Sumatra, Indonesia	*Hylobates agilis*	ZMB records	1	ZMB records	2	—	0	0	Prd
ZMB 6948	R	Borneo	*Pongo pygmaeus*	ZMB records	1	ZMB records	1	—	0	0	Prd
ZMB 6957	L	Borneo	*Pongo pygmaeus*	ZMB records	1	ZMB records	1	—	0	0	—
ZMB 12209	R	Sumatra, Indonesia	*Pongo abelii*	ZMB records	1	ZMB records	1	—	0	0	Prd
ZMB 38607	R	Sumatra, Indonesia	*Pongo abelii*	ZMB records	1	ZMB records	1	—	0	0	—
ZMB 83509	R	Sumatra, Indonesia	*Pongo abelii*	ZMB records	1	ZMB records	1	—	0	0	—
ZMB 83511	L	Sumatra, Indonesia	*Pongo abelii*	ZMB records	1	ZMB records	1	—	0	0	Prd
ZMB 17963	L	Cameroon	*Gorilla gorilla*	ZMB records	1	ZMB records	2	—	1	1	Prd
ZMB 30940	R	Cameroon	*Gorilla gorilla*	ZMB records	1	ZMB records	2	—	0	1	—
ZMB 30941	L	Congo	*Gorilla gorilla*	ZMB records	1	ZMB records	2	—	0	1	Prd
ZMB 31435	R	Cameroon	*Gorilla gorilla*	ZMB records	1	ZMB records	2	—	1	1	—
ZMB 83561	R	Cameroon	*Gorilla gorilla*	ZMB records	1	ZMB records	2	—	0	1	Prd
MPITC 11776	L	Taï, Côte d'Ivoire	*Pan troglodytes verus*	MPI records	1	ZMB records	3	—	1	1	—
MPITC 11800	R	Taï, Côte d'Ivoire	*Pan troglodytes verus*	MPI records	1	ZMB records	3	—	1	1	—
MPITC 11903	R	Taï, Côte d'Ivoire	*Pan troglodytes verus*	MPI records	1	ZMB records	3	—	1	1	Prd
MPITC 13430	R	Taï, Côte d'Ivoire	*Pan troglodytes verus*	MPI records	1	ZMB records	2	—	0	1	—
MPITC 13437	R	Taï, Côte d'Ivoire	*Pan troglodytes verus*	MPI records	1	ZMB records	3	—	0	1	—
KNM-KP 29281	R	Kanapoi, Kenya	*Australopithecus anamensis*	Leakey et al. 1995	1	Ward et al., 2001	—	M	2	1	—
KNM-KP 29286	R	Kanapoi, Kenya	*Australopithecus anamensis*	Leakey et al. 1995	1	Ward et al., 2001	1	M	2	2	—
KNM-KP 53160	L	Kanapoi, Kenya	*Australopithecus anamensis*	Ward et al. 2017	1	Ward et al. 2017	1	M	2	1	—
AL266-1	R	Hadar, Ethiopia	*Australopithecus afarensis*	Johanson et al., 1982	1	Johanson et al., 1982	1	M	1	1	Prd
AL333-10	L	Hadar, Ethiopia	*Australopithecus afarensis*	Johanson et al., 1982	3	Johanson et al., 1982	1	C	2	2	Prd
AL333w-1c	R	Hadar, Ethiopia	*Australopithecus afarensis*	Johanson et al., 1982	2	Johanson et al., 1982	1	M	2	2	—
AL655-1	L	Hadar, Ethiopia	*Australopithecus afarensis*	Kimbel and Delezene, 2009	3	Kimbel and Delezene, 2009	1	—	—	—	—
W8-978	R	Omo, Ethiopia	Indet.	Suwa, 1990	3	Suwa, 1990	—	C	2	1	—
KNM-WT 8556	L	West Turkana, Kenya	Indet.	Brown et al., 2001	1	Brown et al., 2001	1	C	2	1	—
STW 7	L	Sterkfontein, S. Africa	*Australopithecus africanus*	Moggi-Cecchi et al., 2006	3	Moggi-Cecchi et al., 2006	1	C	1	1	Prd
STW 104	L	Sterkfontein, S. Africa	*Australopithecus africanus*	Moggi-Cecchi et al., 2006	1	Moggi-Cecchi et al., 2006	1	C	2	1	—

STW 142	R	Sterkfontein, S. Africa	*Australopithecus africanus*	Moggi-Cecchi et al., 2006	1	Moggi-Cecchi et al., 2006	—	C	2	1	Med
STW 193	R	Sterkfontein, S. Africa	*Australopithecus africanus*	Moggi-Cecchi et al., 2006	2	Moggi-Cecchi et al., 2006	—	—	2	1	—
STW 213	R	Sterkfontein, S. Africa	*Australopithecus africanus*	Moggi-Cecchi et al., 2006	2	Moggi-Cecchi et al., 2006	1	M	2	2	Prd
STW 401	R	Sterkfontein, S. Africa	*Australopithecus africanus*	Moggi-Cecchi et al., 2006	3	Moggi-Cecchi et al., 2006	—	D	2	2	Med
STW 404	R	Sterkfontein, S. Africa	*Australopithecus africanus*	Moggi-Cecchi et al., 2006	1	Moggi-Cecchi et al., 2006	—	C	2	1	Prd
STW 420B	L	Sterkfontein, S. Africa	*Australopithecus africanus*	Moggi-Cecchi et al., 2006	2	Moggi-Cecchi et al., 2006	1	C	2	2	—
STW 498c	L	Sterkfontein, S. Africa	*Australopithecus africanus*	Moggi-Cecchi et al., 2006	1	Moggi-Cecchi et al., 2006	—	C	2	1	—
STS 24	L	Sterkfontein, S. Africa	*Australopithecus africanus*	Brain, 1981	1	Brain, 1981	1	C	1	1	—
STS 51	R	Sterkfontein, S. Africa	*Australopithecus africanus*	Brain, 1981	2	Brain, 1981	1	C	2	1	—
STS 52b	R	Sterkfontein, S. Africa	*Australopithecus africanus*	Dart, 1954	1	Dart, 1954	—	C	2	2	Prd
Taung1	R	Taung, S. Africa	*Australopithecus africanus*	Dart, 1925	1	Dart, 1925	1	M	2	1	—
DNH8	L	Drimolen, S. Africa	*Paranthropus robustus*	Moggi-Cecchi et al., 2010	1	Moggi-Cecchi et al., 2010	1	C	0	1	—
DNH46	R	Drimolen, S. Africa	*Paranthropus robustus*	Moggi-Cecchi et al., 2010	1	Moggi-Cecchi et al., 2010	1	—	—	—	—
DNH51	R	Drimolen, South Africa	*Paranthropus robustus*	Moggi-Cecchi et al., 2010	1	Moggi-Cecchi et al., 2010	—	C	0	1	—
DNH107	L	Drimolen, S. Africa	*Paranthropus robustus*	Museum records	2	Museum records	1	C	0	2	—
SK23	L	Swartkrans, S. Africa	*Paranthropus robustus*	Robinson, 1956	1	Robinson, 1956	—	C	0	0	—
SK30	L	Swartkrans, S. Africa	*Paranthropus robustus*	Robinson, 1956	3	Robinson, 1956	—	—	0	1	—
SK61	R	Swartkrans, S. Africa	*Paranthropus robustus*	Robinson, 1956	1	Robinson, 1956	1	C	0	1	—
SK62	L	Swartkrans, S. Africa	*Paranthropus robustus*	Robinson, 1956	1	Robinson, 1956	1	C	1	2	—
SK63	L	Swartkrans, S. Africa	*Paranthropus robustus*	Robinson, 1956	1	Robinson, 1956	—	—	0	1	—
SK100	R	Swartkrans, S. Africa	*Paranthropus robustus*	Robinson, 1956	3	Oakley, 1977	1	C	0	1	—
SK857	R	Swartkrans, S. Africa	*Paranthropus robustus*	Robinson, 1956	3	Oakley, 1977	1	C	0	0	—
SKW5	R	Swartkrans, S. Africa	*Paranthropus robustus*	Grine and Daegling, 1993	1	Grine and Daegling, 1993	—	C	0	1	Prd
KNM-ER 1820	L	Koobi Fora, Kenya	*Paranthropus boisei*	Wood, 1991	1	Wood, 1991	1	C	—	—	—
KNM-ER 6082	L	Koobi Fora, Kenya	*Paranthropus boisei*	Wood, 1991	3	Wood, 1991	0	C	—	—	—
KNM-ER 15951H	L	Koobi Fora, Kenya	*Paranthropus boisei*	Wood and Leakey, 2011	2	Wood and Leakey, 2011	—	—	0	0	—
KNM-WT 16005	L	West Turkana, Kenya	*Paranthropus boisei*	Leakey and Walker, 1988	1	Leakey and Walker, 1988	1	C	0	1	Prd
L427-7	R	Omo, Ethiopia	*Paranthropus boisei*	Suwa et al., 1996	1	Suwa et al., 1996	0	—	2	2	—
KNM-ER 806E	L	Koobi Fora, Kenya	*Homo* sp. (*Homo ergaster*)	Wood, 1991	2	Wood, 1991	—	—	2	0	—
KNM-ER 5431E	L	Koobi Fora, Kenya	Indet.	Wood, 1991	2	Wood, 1991	2	C	—	—	—
SKX 21204	R	Swartkrans, S. Africa	*Homo* sp.	Grine, 1989	1	Grine, 1989	1	C	2	1	—
STW 151	R	Sterkfontein, S. Africa	Indet.	Moggi-Cecchi et al., 1998	1	Moggi-Cecchi et al., 1998	1	C	2	2	—
U.W. 101-0010	R	Rising Star, S. Africa	*Homo naledi*	Berger et al. 2015	1	Berger et al. 2015	—	C	1	1	—
U.W. 101-144	L	Rising Star, S. Africa	*Homo naledi*	Berger et al. 2015	3	Berger et al. 2015	1	C	1	0	—

U.W. 101-377[b]	R	Rising Star, S. Africa	*Homo naledi*	Berger et al. 2015	1	Berger et al. 2015	—	—	—	—	—
U.W. 101-506[b]	R	Rising Star, S. Africa	*Homo naledi*	Berger et al. 2015	3	Berger et al. 2015	—	—	—	—	—
U.W. 101-850	R	Rising Star, S. Africa	*Homo naledi*	Berger et al. 2015	3	Berger et al. 2015	—	—	1	1	—
U.W. 101-889	L	Rising Star, S. Africa	*Homo naledi*	Berger et al. 2015	3	Berger et al. 2015	1	C	1	1	—
U.W. 101-1261	R	Rising Star, S. Africa	*Homo naledi*	Berger et al. 2015	1	Berger et al. 2015	1	C	1	1	Prd
U.W. 101-1565	L	Rising Star, S. Africa	*Homo naledi*	Berger et al. 2015	1	Berger et al. 2015	1	C	0	1	—
U.W. 102-0023	R	Rising Star, S. Africa	*Homo naledi*	Hawks et al. 2017	3	Hawks et al. 2017	—	—	1	1	—
Cave of hearths	R	Cave of hearths, S. Africa	Indet.	Tobias, 1971	1	Tobias, 1971	1	M	0	0	—
Mauer 1	R	Mauer, Germany	*Homo heidelbergensis*	Schoetensack, 1908	1	Schoetensack, 1908	—	MD	0	0	—
Combe-Grenal I	R	Combe Grenal, France	*Homo neanderthalensis*	Garralda and Vandermeersch, 2000	1	Garralda and Vandermeersch, 2000	1	C	1	0	—
KRP 51	R	Krapina, Croatia	*Homo neanderthalensis*	Radovčić, 1988	1	Radovčić, 1988	1	C	1	1	—
KRP 52	L	Krapina, Croatia	*Homo neanderthalensis*	Radovčić, 1988	1	Radovčić, 1988	1a	C	1	0	—
KRP 54	L	Krapina, Croatia	*Homo neanderthalensis*	Radovčić, 1988	1	Radovčić, 1988	1a	M	0	0	—
KRP 55	L	Krapina, Croatia	*Homo neanderthalensis*	Radovčić, 1988	1	Radovčić, 1988	1	C	0	0	—
KRP 58	R	Krapina, Croatia	*Homo neanderthalensis*	Radovčić, 1988	1	Radovčić, 1988	—	C	1	0	—
KRP D27	L	Krapina, Croatia	*Homo neanderthalensis*	Radovčić, 1988	2	Radovčić, 1988	—	C	1	0	—
KRP D28	R	Krapina, Croatia	*Homo neanderthalensis*	Radovčić, 1988	2	Radovčić, 1988	—	M	0	0	—
KRP D29	R	Krapina, Croatia	*Homo neanderthalensis*	Radovčić, 1988	2	Radovčić, 1988	—	M	0	0	—
KRP D33	L	Krapina, Croatia	*Homo neanderthalensis*	Radovčić, 1988	2	Radovčić, 1988	1a	C	0	0	—
KRP D34	R	Krapina, Croatia	*Homo neanderthalensis*	Radovčić, 1988	3	Radovčić, 1988	—	—	1	1	Prd
KRP D111	L	Krapina, Croatia	*Homo neanderthalensis*	Radovčić, 1988	3	Radovčić, 1988	1	M	1	1	—
KRP D114	L	Krapina, Croatia	*Homo neanderthalensis*	Radovčić, 1988	2	Radovčić, 1988	1a	C	1	0	—
SCLA 4A 6	R	Scladina, Belgium	*Homo neanderthalensis*	Toussaint et al., 1998	2	Toussaint et al., 1998	1	C	0	0	—
Qafzeh 10	R	Qafzeh, Israel	Fossil *Homo sapiens*	Vandermeersch, 1981	1	Vandermeersch, 1981	1	C	0	0	—
Qafzeh 11	R	Qafzeh, Israel	Fossil *Homo sapiens*	Vandermeersch, 1981	1	Vandermeersch, 1981	1	M	0	0	—
ULAC 1	R	Anatomical collection	*Homo sapiens*	ULAC records	1	ULAC records	—	C	0	0	—
ULAC 58	L	Anatomical collection	*Homo sapiens*	ULAC records	1	ULAC records	1	M	0	0	—
ULAC 58[b]	R	Anatomical collection	*Homo sapiens*	ULAC records	1	ULAC records	—	—	—	—	
ULAC 66	L	Anatomical collection	*Homo sapiens*	ULAC records	1	ULAC records	0	MD	0	0	Prd
ULAC 74	L	Anatomical collection	*Homo sapiens*	ULAC records	1	ULAC records	—	C	0	1	—
ULAC 171	L	Anatomical collection	*Homo sapiens*	ULAC records	1	ULAC records	0	MD	0	0	—
ULAC 522	L	Anatomical collection	*Homo sapiens*	ULAC records	1	ULAC records	—	C	0	0	—
ULAC 536	R	Anatomical collection	*Homo sapiens*	ULAC records	1	ULAC records	1	C	0	0	Prd
ULAC 607	R	Anatomical collection	*Homo sapiens*	ULAC records	1	ULAC records	—	C	0	0	—

ULAC 790	L	Anatomical collection	*Homo sapiens*	ULAC records	1	ULAC records	*	MD	0	0	—
ULAC 797	R	Anatomical collection	*Homo sapiens*	ULAC records	1	ULAC records	0	C	0	0	—
ULAC 801	L	Anatomical collection	*Homo sapiens*	ULAC records	1	ULAC records	1	D	1	1	—
ULAC 806	L	Anatomical collection	*Homo sapiens*	ULAC records	1	ULAC records	0	MD	0	0	—

Abbreviations: TC = transverse crest form; see main text for typology (* = EDJ preserved but transverse crest form could not be determined—see main text for details); MR = marginal ridge (C = continuous; M = mesially discontinuous; D = distally discontinuous; MD = mesially and distally discontinuous); MBG = mesial buccal groove (0 = absent; 1 = minor; 2 = marked; for description of these character states, see main text); DBG = distal buccal groove (character states as for MBG); Recon? = specimens with reconstructed dentine horns (Prd = protoconid reconstructed; Med = metaconid reconstructed).

[a] Position basis: 1 = In jaw; 2 = associated dentition; 3 = based on morphology.

[b] Antimere specimens that are not included in analyses, but are discussed in the main text.

SOM Table S2

Additional information on the modern human sample, as listed in the records of the Anatomical Collection of the University of Leipzig

Specimen number	Region	Age	Sex
ULAC_1	Germany/Rheinland	Adult	Male
ULAC_58	Norway	Adult	Male
ULAC_66	Norway/Sweden	Adult	Female
ULAC_74	Italy (Etruscan, Tarquinii)	Adult	Male
ULAC_171	Italy (Etruscan, Tarquinii)	Adult	Male
ULAC_522	Egypt (Thebes)	Adult	Male
ULAC_536	Egypt (Thebes)	Adult	Male
ULAC_607	Egypt (Thebes)	Adult	Male
ULAC_790	Africa (Americans/New Orleans)	Adult	Male
ULAC_797	Africa (Americans/New Orleans)	Adult	Male
ULAC_801	Africa (Americans/New Orleans)	Adult	Female
ULAC_806	Africa (Americans/New Orleans)	Adult	Male

SOM Table S3

Results of the inter- and intra-observer error tests for the four P_3 discrete traits scored.

Trait	Inter-observer agreement (%)	Intra-observer agreement (%)
Transverse crest	100	98
Marginal ridge	92	99
Mesial buccal groove	96	89
Distal buccal groove	88	93

SOM References

Berger, L.R., Hawks, J., de Ruiter, D.J., Churchill, S.E., Schmid, P., Delezene, L.K., Kivell, T.L., Garvin, H.M., Williams, S.A., DeSilva, J.M., Skinner, M.M., Musiba, C.M., Cameron, N., Holliday, T.W., Harcourt-Smith, W., Ackermann, R.R., Bastir, M., Bogin, B., Bolter, D., Brophy, J., Cofran, Z.D., Congdon, K.A., Deane, A.S., Dembo, M., Drapeau, M., Elliott, M.C., Feuerriegel, E.M., Garcia-Martinez, D., Green, D.J., Gurtov, A., Irish, J.D., Kruger, A., Laird, M.F., Marchi, D., Meyer, M.R., Nalla, S., Negash, E.W., Orr, C.M., Radovcic, D., Schroeder, L., Scott, J.E., Throckmorton, Z., Tocheri, M.W., VanSickle, C., Walker, C.S., Wei, P., Zipfel, B., 2015. *Homo naledi*, a new species of the genus *Homo* from the Dinaledi Chamber, South Africa. eLife 4, e09560.

Brain, C.K., 1981. The Hunters or the Hunted?: An Introduction to African Cave Taphonomy. University of Chicago Press, Chicago.

Brown, B., Brown, F.H., Walker, A., 2001. New hominids from the Lake Turkana basin, Kenya. Journal of Human Evolution 41, 29-44.

Dart, R.A., 1925. *Australopithecus africanus* the man-ape of South Africa. Nature 115, 195–199.

Dart, R.A., 1954. The second, or adult, female mandible of *Australopithecus prometheus*. American Journal of Physical Anthropology 12, 313-344.

Garralda, M.-D., Vandermeersch, B., 2000. Les Néandertaliens de la grotte de Combe-Grenal (Domme, Dordogne, France)/The Neanderthals from Combe-Grenal cave (Domme, Dordogne, France). Paléo 12, 213-259.

Grine, F.E., 1989. New hominid fossils from the Swartkrans Formation (1979–1986 excavations): craniodental specimens. American Journal of Physical Anthropology 79, 409-449.

Grine, F.E., Daegling, D.J., 1993. New mandible of *Paranthropus robustus* from Member 1, Swartkrans Formation, South Africa. Journal of Human Evolution 24, 319-333.

Hawks, J., Elliott, M., Schmid, P., Churchill, S.E., Ruiter, D.J.d., Roberts, E.M., Hilbert-Wolf, H., Garvin, H.M., Williams, S.A., Delezene, L.K., Feuerriegel, E.M., Randolph-Quinney, P., Kivell, T.L., Laird, M.F., Tawane, G., DeSilva, J.M., Bailey, S.E., Brophy, J.K., Meyer, M.R., Skinner, M.M., Tocheri, M.W., VanSickle, C., Walker, C.S., Campbell, T.L., Kuhn, B., Kruger, A., Tucker, S., Gurtov, A., Hlophe, N., Hunter, R., Morris, H., Peixotto, B., Ramalepa, M., Rooyen, D.v., Tsikoane, M., Boshoff, P., Dirks, P.H.G.M., Berger, L.R., 2017. New fossil remains of *Homo naledi* from the Lesedi Chamber, South Africa. eLife 6, e24232.

Johanson, D.C., White, T.D., Coppens, Y., 1982. Dental remains from the Hadar Formation, Ethiopia: 1974–1977 collections. American Journal of Physical Anthropology 57, 545-603.

Kimbel, W.H., Delezene, L.K., 2009. "Lucy" redux: A review of research on *Australopithecus afarensis*. American Journal of Physical Anthropology 140, 2-48.

Kimbel, W.H., Johanson, D.C., Rak, Y., 1994. The first skull and other new discoveries of *Australopithecus afarensis* at Hadar, Ethiopia. Nature 368, 449.

Leakey, M.G., Feibel, C.S., McDougall, I., Walker, A., 1995. New four-million-year-old hominid species from Kanapoi and Allia Bay, Kenya. Nature 376, 565.

Leakey, R., Walker, A., 1988. New *Australopithecus boisei* specimens from east and west Lake Turkana, Kenya. American Journal of Physical Anthropology 76, 1-24.

Moggi-Cecchi, J., Grine, F.E., Tobias, P.V., 2006. Early hominid dental remains from Members 4 and 5 of the Sterkfontein Formation (1966–1996 excavations): catalogue, individual associations, morphological descriptions and initial metrical analysis. Journal of Human Evolution 50, 239-328.

Moggi-Cecchi, J., Menter, C., Boccone, S., Keyser, A., 2010. Early hominin dental remains from the Plio-Pleistocene site of Drimolen, South Africa. Journal of Human Evolution 58, 374-405.

Moggi-Cecchi, J., Tobias, P.V., Beynon, A., 1998. The mixed dentition and associated skull fragments of a juvenile fossil hominid from Sterkfontein, South Africa. American Journal of Physical Anthropology 106, 425-465.

Oakley, K.P., Campbell, B.G., Molleson, T.I., Museum, B., 1977. Catalogue of Fossil Hominids. Part I: Africa. Trustees of the British Museum (Natural History), London.

Radovčić, J., 1988. The Krapina Hominids: An Illustrated Catalog of Skeletal Collection. Mladost, Zagreb.

Robinson, J.T., 1956. The Dentition of Australopithecinae. Transvaal Museum, Pretoria.

Schoetensack, O., 1908. Der Unterkiefer des *Homo heidelbergensis* aus den Sanden von Mauer bei Heidelberg. Ein Beitrag zur Paläontologie des Menschen. Zeitschrift für Induktive Abstammungs-und Vererbungslehre 1, 408-410.

Suwa, G., 1990. A Comparative analysis of hominid dental remains from the Sungura and Usno Formations. Omo Valley, Ethiopia. Ph.D. Dissertation, University of California, Berkeley.

Suwa, G., White, T.D., Howell, F.C., 1996. Mandibular postcanine dentition from the Shungura Formation, Ethiopia: Crown morphology, taxonomic allocations, and Plio-Pleistocene hominid evolution. American Journal of Physical Anthropology 101, 247-282.

Tobias, P.V., 1971. Human skeletal remains from the Cave of Hearths, Makapansgat, northern Transvaal. American Journal of Physical Anthropology 34, 335-367.

Toussaint, M., Otte, M., Bonjean, D., Bocherens, H., Falguères, C., Yokoyama, Y., 1998. Les restes humains néandertaliens immatures de la couche 4A de la grotte Scladina (Andenne, Belgique). Comptes Rendus de l'Académie des Sciences Paris 326, 737-742.

Vandermeersch, B., 1981. Les Hommes Fossiles de Qafzeh (Israël). Editions du Centre National de la Recherche Scientifique, Paris.

Walker, A., Leakey, R.E. (Eds.), 1993. The Nariokotome *Homo erectus* Skeleton. Harvard University Press, Cambridge.

Ward, C., Manthi, F., Plavcan, J., 2017. New fossils of *Australopithecus anamensis* from Kanapoi, West Turkana, Kenya (2012–2015). Journal of Human Evolution. https://doi.org/10.1016/j.jhevol.2017.07.008

Ward, C.V., Leakey, M.G., Walker, A., 2001. Morphology of *Australopithecus anamensis* from Kanapoi and Allia Bay, Kenya. Journal of Human Evolution 41, 255-368.

Wood, B., 1991. Koobi Fora Research Project Volume 4: Hominid Cranial Remains from Koobi Fora. Clarendon, Oxford.

Wood, B., Leakey, M., 2011. The Omo-Turkana Basin fossil hominins and their contribution to our understanding of human evolution in Africa. Evolutionary Anthropology 20, 264-292.